iScience

CellPress

Article

Genomic Approaches Reveal an Endemic Subpopulation of Gray Wolves in Southern China

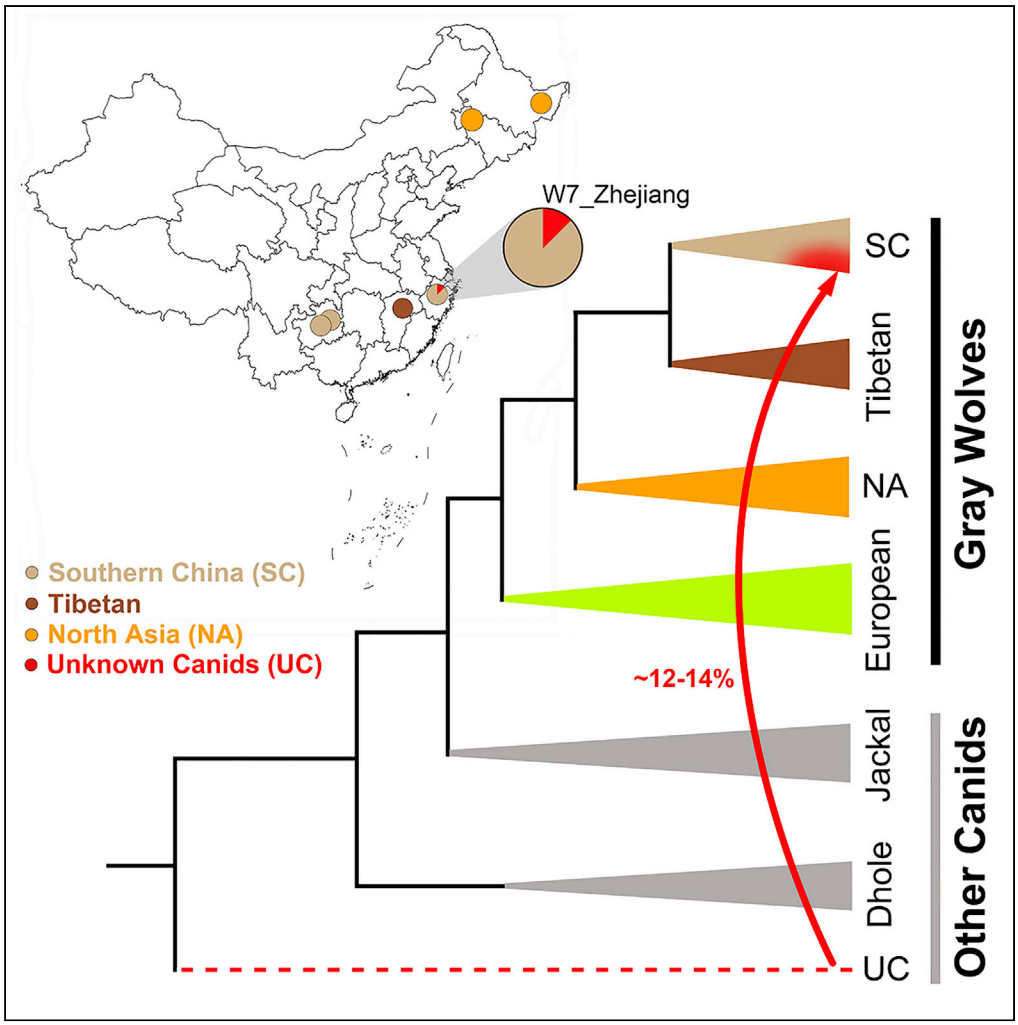

Guo-Dong Wang, Ming Zhang, Xuan Wang, ..., Lu Wang, Qiaomei Fu, Ya-Ping Zhang

fuqiaomei@ivpp.ac.cn (Q.F.)
zhangyp@mail.kiz.ac.cn (Y.-P.Z.)

HIGHLIGHTS

Gray wolves from South China derive from a single lineage

A Zhejiang wolf shows admixture (~12%–14%) from a deeply diverged canid species

Lowland gray wolf shows close genetic relationship to Tibetan Plateau gray wolves

Wang et al., iScience *20*, 110–118
October 25, 2019
https://doi.org/10.1016/j.isci.2019.09.008

iScience

CellPress

Article

Genomic Approaches Reveal an Endemic Subpopulation of Gray Wolves in Southern China

Guo-Dong Wang,[1,2,9] Ming Zhang,[3,4,5,9] Xuan Wang,[1,2,5] Melinda A. Yang,[3,4] Peng Cao,[3] Feng Liu,[3] Heng Lu,[6] Xiaotian Feng,[3] Pontus Skoglund,[7] Lu Wang,[8] Qiaomei Fu,[3,4,5,*] and Ya-Ping Zhang[1,2,10,*]

SUMMARY

Although gray wolves (*Canis lupus*) are one of the most widely distributed terrestrial mammals, their origins in China are not well understood. We sequenced six specimens from wolf skins, showing that gray wolves from Southern China (SC) derive from a single lineage, distinct from gray wolves from the Tibetan Plateau and Northern China, suggesting that SC gray wolves may form a distinct subpopulation. Of SC gray wolves, one wolf from Zhejiang carries a genetic component from a canid and had gene flow from a population related to or further diverged from wolves than the dhole. This may indicate that interspecific gene flow likely played an important role in shaping the speciation patterns and population structure in the genus *Canis*. Our study is the first to survey museum gray wolves' genomes from Southern China, highlighting how sequencing the paleogenome from museum specimens can help us to study extinct species.

INTRODUCTION

The place of origin for domestic dogs (*Canis lupus familiaris*) remains a controversial question for the scientific community despite many efforts at studying dog domestication (Botigué et al., 2017; Frantz et al., 2016; Liu et al., 2018; Shannon et al., 2015; Thalmann et al., 2013; Vonholdt et al., 2010; Wang et al., 2016a). Geographic distribution, population structure, and genomic features of wild ancestors are essential factors to determine sources of domestication (Wang et al., 2016b). Gray wolves (*Canis lupus*) are the closest wild relative of dogs, and they are also one of the most widely distributed terrestrial mammals, originally inhabiting major parts of Eurasia, North America, and North Africa (Loog et al., 2018; Wilson and Reeder, 2005; Young et al., 1944). Previous studies suggested that gray wolves have a complex history (vonHoldt et al., 2011; Wayne et al., 1992), with subpopulation structure related to local niches (Carmichael et al., 2001; Geffen et al., 2004; Pilot et al., 2006, 2014) and long-term genetic admixture not only with dogs (Freedman et al., 2014; Liu et al., 2018) but also with coyotes (Fan et al., 2016; Monzon et al., 2014; Pilot et al., 2014; vonHoldt et al., 2016; vonHoldt et al., 2011). In China, gray wolves were distributed across the mainland, including most southern regions (Smith and Xie, 2014; Wang et al., 2016b). Genomic approaches using gray wolf specimens from Southern China (SC) may help to shed new light on the demographic history of gray wolves and domestic dogs.

RESULTS AND DISCUSSION

From two natural history museums in China, we obtained six historical gray wolf skin samples collected from Mainland China (Figures 1A and S1 and Table 1, detailed description in Wang et al., 2016b). More details for the samples are shown in the methods (Transparent Methods). As skin samples were treated with chemical reagents and underwent special processing for preservation during storage and exhibition in museums, we used a modified ancient DNA (aDNA) protocol (Dabney et al., 2013) to retrieve genetic material from the skin samples. In total, 35 genomic libraries were produced for these six samples using a double-stranded library preparation protocol (Kircher et al., 2012; Meyer and Kircher, 2010), and each was treated with uracil-DNA glycosylase and endonuclease (Endo VIII) to remove characteristic aDNA deamination (Briggs et al., 2007) (Table S1). We sequenced the libraries using 2×150-bp reads on an Illumina HiSeq X platform.

We included 103 canids from previous studies (Auton et al., 2013; Botigué et al., 2017; Decker et al., 2015; Freedman et al., 2014; Marsden et al., 2016; Skoglund et al., 2015; Tang et al., 2019; vonHoldt et al., 2016;

[1]State Key Laboratory of Genetic Resources and Evolution, Kunming Institute of Zoology, Chinese Academy of Sciences, Kunming 650223, China

[2]Center for Excellence in Animal Evolution and Genetics, Chinese Academy of Sciences, Kunming 650223, China

[3]Key Laboratory of Vertebrate Evolution and Human Origins of Chinese Academy of Sciences, IVPP, CAS, Beijing 100044, China

[4]Center for Excellence in Life and Paleoenvironment, Chinese Academy of Sciences, Beijing 100044, China

[5]University of Chinese Academy of Sciences, Beijing 100049, China

[6]Department of Molecular and Cell Biology, School of Life Sciences, University of Science and Technology of China, Hefei 230026, China

[7]The Francis Crick Institute, London NW1 1AT, UK

[8]State Key Laboratory for Conservation and Utilization of Bio-Resources in Yunnan, Yunnan University, Kunming 650091, China

[9]These authors contributed equally

[10]Lead Contact

*Correspondence: fuqiaomei@ivpp.ac.cn (Q.F.), zhangyp@mail.kiz.ac.cn (Y.-P.Z.)

https://doi.org/10.1016/j.isci.2019.09.008

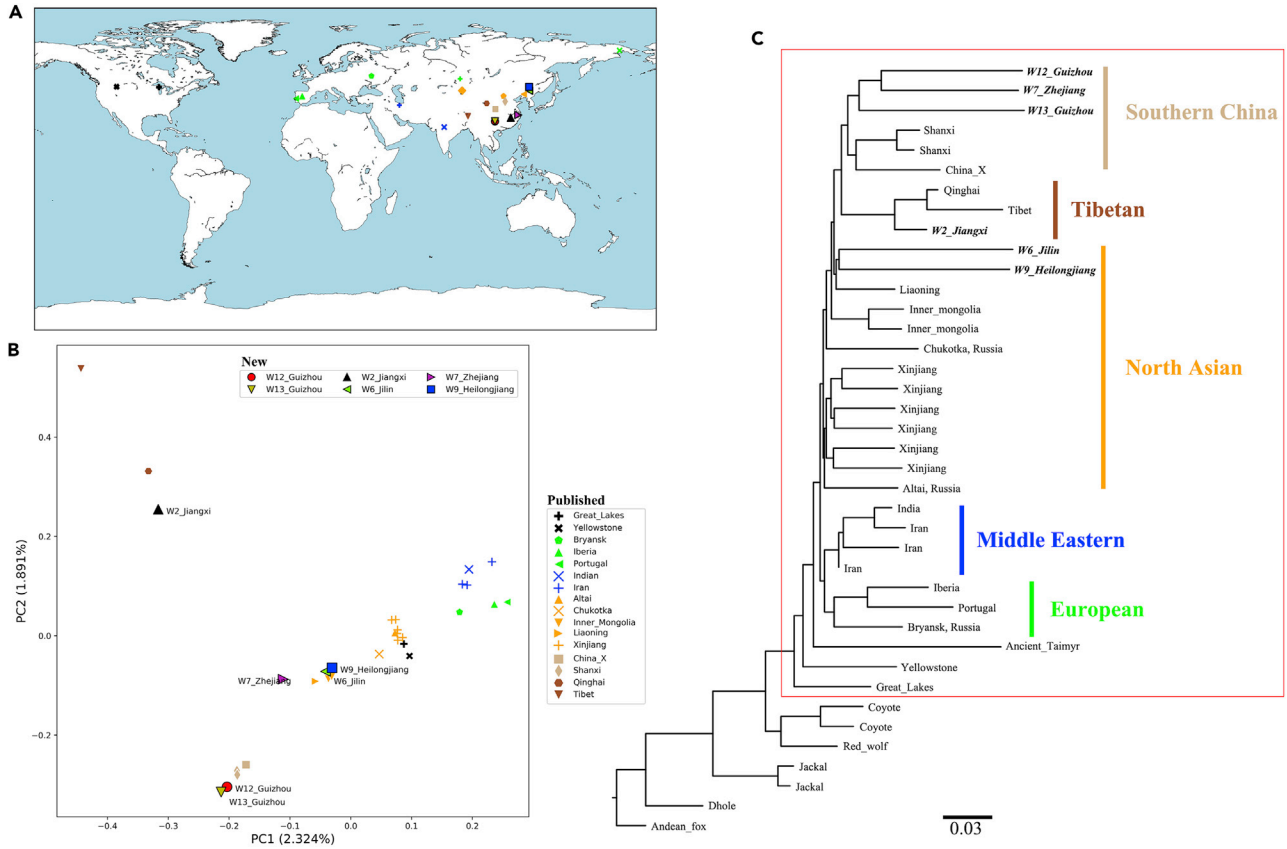

Figure 1. Geographic Locations, Population Structure of 31 Gray Wolves, and Phylogeny of 39 Canids

(A and B) (A) Geographic locations, where the key is shared with the principal-component analysis in (B). In (B), the label "New" represents the six samples sequenced in the study, and the label "Published" represents 25 samples from previous studies.

(C) The maximum likelihood tree of 39 canids, where the Andean fox is used as an outgroup. All the gray wolves are in the red line, and the newly sequenced individuals are marked in bold and italics.

Wang et al., 2019a; Wang et al., 2016a; Wang et al., 2013; Wang et al., 2019b; Zhang et al., 2014), including an ancient gray wolf, Taimyr; 25 modern gray wolves chosen from regions overlapping their current ranges; 70 domestic dogs from all over the world; two jackals; two coyotes; one red wolf; one dhole; and one Andean fox (Figure 1, Table S2). We obtained 13.74 million SNPs, including 4.25 million transversions for further analysis (Transparent Methods).

All samples were sequenced to ~0.15- to 15.3-fold average coverage except for the Jiangxi wolf (W2_Jiangxi), which was sequenced to 37.00-fold coverage (Table 1). Because most samples have low average coverage, we focused on SNPs previously found for modern canids (Marsden et al., 2016; Wang et al., 2016a), for which we called haploid alleles using randomly chosen sequence reads for every sample except W2_Jiangxi. We applied a filter where we ignored fragments with length less than 30, ignored the first and last two base pairs of each fragment, and required a base pair quality higher than 20 and mapping quality of at least 30. For the high-coverage W2_Jiangxi (Table 1) as well as the two medium-coverage Guizhou wolves (W12_Guizhou and W13_Guizhou), we called heterozygotes using the software GATK with the Unified Genotyper parameter to determine diploid calls (DePristo et al., 2011). Results using diploid calls for W12_Guizhou and W13_Guizhou are similar to results using random calls without heterozygous sites.

Phylogeny and Population Structure

To investigate the relationship of the newly sampled individuals to wolf and dog populations, we calculated pairwise allele-sharing distances among all pairs of wolf and dog populations. We applied a principal-components analysis (PCA) to the resulting pairwise distance matrix using SMARTPCA (version: 13050)

Sample ID	Coverage	SNPs	Sources	Location
W6_Jilin	1.87	6,890,236	National Zoological Museum of China, Beijing, China	Jilin
W7_Zhejiang	0.15	1,866,574		Zhejiang
W9_Heilongjiang	1.61	5,438,606		Heilongjiang
W12_Guizhou	15.33	12,688,043	Kunming Natural History Museum of Zoology, Yunnan, China	Guizhou
W13_Guizhou	12.39	12,968,150		Guizhou
W2_Jiangxi	37.00	13,528,667		Jiangxi

Table 1. Information on Samples Sequenced in This Study

(Patterson et al., 2006). The first principal component distinguishes between gray wolf and dog populations, whereas the second principal component distinguishes between East Asian and European dogs (Figure S2), consistent with previous studies (Frantz et al., 2016; Vonholdt et al., 2010; Wang et al., 2016a). To obtain increased resolution, we redid the PCA excluding dog populations (Figure 1B). The resulting PCA shows that the two new Guizhou wolves (W12_Guizhou and W13_Guizhou) cluster with a Chinese wolf from the San Diego Zoo, whose origin is not recorded (labeled as "China_X" in this study) (Freedman et al., 2014), and two gray wolves from Shanxi, China, sampled in 1988 near the border of SC (Wang et al., 2016a). We also find that the new Jilin and Heilongjiang wolves (W6_Jilin and W9_Heilongjiang) cluster with gray wolves from Inner Mongolia and Liaoning. The new Jiangxi wolf (W2_Jiangxi) is closest to the Qinghai wolf, whereas the Zhejiang wolf (W7_Zhejiang) is closest to the cluster containing the gray wolves from Inner Mongolia and Liaoning (Figure S1).

We constructed a maximum likelihood (ML) tree (Figure 1C) and a neighbor-joining tree with only wolves (Figure S3), from which we further find that the Zhejiang wolf forms a clade with the Guizhou, Shanxi, and China_X wolves (Figure 1C). We define these gray wolves as the gray wolves from SC and find that they are most closely related to the Qinghai, Tibet, and Jiangxi wolves, where the Tibetan gray wolf (*Canis lupus chanco*) is a gray wolf subspecies that occupies habitats on the Qinghai-Tibet Plateau (Pocock, 1941) and possesses adaptations to high-altitude environments (Zhang et al., 2014). Other gray wolves from Northern Asia (NA, e.g., W6_Jilin, W9_Heilongjiang, and Liaoning) form a clade with the SC and Tibetan gray wolves relative to other NA, Middle Eastern, and European gray wolves that form a distinct clade with each other. The 35,000-year-old wolf from the Taimyr Peninsula in Northern Siberia joins at the base of the Eurasian wolf phylogeny, and American wolves separate the earliest from other wolves, consistent with Freedman et al. (2014).

We used TreeMix (v. 1.13) (Pickrell and Pritchard, 2012) to investigate the genetic relationship between historical and present-day wolves. TreeMix determines population structure using ML trees and allows for both population splits and potential gene flow by using genome-wide allele frequency data and a Gaussian approximation of genetic drift. The ML tree (Figure S4) without admixture (m = 0) is consistent with previous patterns, wherein gray wolves from East Asia form three groups: Guizhou and Zhejiang wolves form a clade with Shanxi and China_X wolves, the Jiangxi wolf forms a clade with Tibet and Qinghai wolves, and Jilin and Heilongjiang wolves, like other NA wolves, are outgroup to SC and Tibetan wolves. All three of these groups form a clade relative to non-Asian wolves.

We measured the shared genetic drift between each newly sequenced individual (X) and other dogs and wolves (Y) since their separation from an outgroup, Dhole, using f_3(*X*, *Y*; *Dhole*) (Raghavan et al., 2014; Wang et al., 2019a) and found a similar pattern as above, where the Zhejiang wolf shares the most genetic drift with gray wolves from Guizhou (Figure S5). We then used D-statistics (Patterson et al., 2012) of the form *D*(*Fox*, *Test*; *X*, *Y*), where X and Y are previously published wolves, to formally test the relationship these historical wolves have with different wolf populations. For Guizhou and Zhejiang wolves, we find that they share more alleles with the SC gray wolves (Shanxi and China_X) than with all other wolves, as *D*(*Fox*, *W12_Guizhou/W13_Guizhou/W7_Zhejiang*; *X*, *SC*) > 0 (9.8 < Z < 38.0, Table S3). The Jiangxi wolf shares more allele with the Tibet and Qinghai gray wolves than with other wolves, as *D*(*Fox*, *W2_Jiangxi*; *X*, *Tibet/Qinghai*) > 0 (11.9 < Z < 27.6, Table S3), whereas Jilin and Heilongjiang wolves share the most alleles with NA gray wolves. These results support our above-mentioned analyses, again grouping the Guizhou

and Zhejiang wolves with the SC wolves, the Jiangxi wolf with the Tibetan wolves, and the Jilin and Heilongjiang wolves with the NA wolves.

In summary, our results revealed that the lowland Chinese wolves (Fan et al., 2016) consisted of two major populations: SC and NA wolves. Gray wolves from Zhejiang and Guizhou group most closely with and share the most genetic drift with SC wolves, which includes present-day populations in Shanxi and China_X. The Jilin and Heilongjiang gray wolves share the most genetic similarity to the NA gray wolves, which is the other clade in Northern China and Eastern Russia.

Testing for Admixture in Gray Wolves

Using *D*(*Fox*, *X*; *Test*, *Y*), we find that all gray wolves (X) share more alleles with the Guizhou, Jilin, and Heilongjiang wolves (Test) than with the gray wolves from Tibet and Qinghai, i.e., *D*(*Fox*, *X*; *Test*, *Qinghai/Tibet*) < 0 (Table S5). The Jiangxi wolf shares more alleles with the Tibet and Qinghai wolves than with the other wolves (Table S3), and here, we find that the Tibet and Qinghai wolves share more alleles with the Jiangxi wolf, i.e., *D*(*Fox*, *Qinghai/Tibet*; *W2_Jiangxi*, *X*) < 0 ($-34.5 < Z < -15.4$, Table S5), emphasizing that the Jiangxi, Tibet, and Qinghai wolves form a clade. However, whereas *D*(*Fox*, *X*; *W2_Jiangxi*, *Qinghai*)~ 0 ($-2.3 < Z < 1.8$, Table S5), indicating a symmetric relationship as expected for the Jiangxi and Qinghai wolves forming a clade, we observe *D*(*Fox*, *X*; *W12_Jiangxi*, *Tibet*) < 0 (Table S5), suggesting that the Jiangxi wolf has a connection to other wolves relative to the Tibetan wolf. Thus, we observe that the Tibet and Qinghai gray wolves act as an outgroup to most SC and NA gray wolf populations, and although the Jiangxi wolf forms a clade with the Tibet and Qinghai gray wolves, the Jiangxi wolf also shows connections to non-Tibetan wolf populations. To test for admixture between the SC, NA, and Tibetan wolves, we used *f3*(*Test*; *X*, *Y*), where a significantly negative value ($Z < -3$) suggests that the Test population is a mixture of ancestry related to X and Y, two other wolf populations. Testing all combinations as both a source population and the admixed population, we found that *f3*(*W12_Jiangxi/Qinghai*; *Tibetan*, *SC/NA*) < 0 ($-19.101 < Z < -9.141$, Table S4), suggesting that both the Jiangxi and Qinghai wolves show evidence of ancestry from populations related to both Tibetan and SC gray wolves, explaining why the Jiangxi gray wolf shares a connection to non-Tibetan gray wolf populations.

In contrast to all other gray wolves from China, the Zhejiang wolf shows a markedly different pattern, where all other wolf populations, including the Tibetan and Qinghai gray wolves and more distantly related wolves from further west, form a clade with each other relative to the Zhejiang wolf. That is, we observe that *D*(*Fox*, *X*; *W7_Zhejiang*, *Y*) > 0 ($8.0 < Z < 81.3$, Table S5), where X and Y are all other gray wolves, including the Taimyr. Earlier, we found that *D*(*Fox*, *W7_Zhejiang*; *X*, *Shanxi/China_X*) > 0 (Table S3), indicating that the Zhejiang wolf shows connections to the wolves from Shanxi and China_X. These results suggest that the Zhejiang wolf shows a close relationship to gray wolves from Shanxi and China_X, but that this wolf also possesses an ancestral component that is older than the common ancestral population of the Taimyr and all other gray wolves. The error rate for the Zhejiang wolf (0.4%) is higher than that estimated for other wolves sequenced in this study (0.1%–0.2%), likely because of its low coverage (Table 1). After simulating an error rate similar to that observed for the Zhejiang wolf in these other wolves, we find that our results remain consistent with our previous results. That is, the Zhejiang wolf shows a distinct pattern from that observed in other wolves for both lower and higher error rates.

We use the genomic data from canids typically outgroup to all wolves and dogs, the Dhole, Jackal, Coyote, and Red wolf, to understand how deeply the old component found in the Zhejiang wolf separated from other canid populations. Other canids separated from wolf populations very early, with the Dhole diverging earliest, followed by the Jackal and most recently the Coyote (Lindblad-Toh et al., 2005; Macdonald and Sillero-Zubiri, 2004; Wayne et al., 1997). The Red wolf is genetically very similar to the Coyote and shows substantial gene flow from gray wolves (vonHoldt et al., 2016; vonHoldt et al., 2011). First, comparing the Jackal to wolves (X) and the Coyote, we find that for all wolves but the Zhejiang wolf, *D*(*Fox*, *Jackal*; *X*, *Coyote*) ranges from -0.042 to -0.017 ($-16.5 < Z < -6.4$, Table S6), indicating a connection between the Jackal and gray wolves. We find the reverse for the Zhejiang wolf, however, where the Jackal shares more alleles with the Coyote than with the Zhejiang wolf, i.e., *D*(*Fox*, *Jackal*; *W7_Zhejiang*, *Coyote*) $=0.134$ ($Z = 34.1$, Table S6). We find similar results replacing the Coyote with the Red wolf. The large contrast between the results for the Zhejiang wolf compared with other gray wolves suggests that the old component came from a population that diverged deeply in the past, who separated before the common ancestor of jackals and coyotes.

We also observe that for all gray wolves, we find *D*(*Fox*, *Dhole*; *X*, *Jackal*) > 0 (Table S6), suggesting that gray wolves share a deep lineage older than the separation of the Jackal and Dhole or that there is a direct genetic connection between the Jackal and Dhole. However, whereas D ranges from 0.004 to 0.028 ($4.5 < Z < 7.9$, Table S6) for most gray wolves, using the Zhejiang wolf greatly increases the D value to 0.117 ($Z = 20.2$, Table S6). We find that *D*(*Fox*, *Dhole*; *W7_Zhejiang*, *Jackal*) remains significantly positive ($Z = 12.2$) using only transversions, suggesting that the result for the Zhejiang wolf is not related to aDNA damage and likely reflects an unusual admixture history. If the Zhejiang wolf was no different from other gray wolves, especially the two Guizhou individuals to which they share the closest relationship (Table S5), we would expect to find that *D*(*Fox*, *Dhole*; *X*, *Zhejiang*)∼*0*, which would indicate that the Zhejiang wolf and other gray wolves are similarly related to the Dhole. However, we observe that *D*(*Fox*, *Dhole*; *X*, *W7_Zhejiang*) < 0 ($-22.4 < Z < -11.7$, Table S6), indicating that the Dhole shares more alleles with other gray wolves than with the Zhejiang wolf. These patterns suggest that the ancestral component found in the Zhejiang wolf came from a population that diverged earlier than the common ancestor of the Jackal and Dhole, which is older than the separation of the Jackal and Dhole from wolves, suggesting that the Zhejiang wolf possesses very deep ancestry not found in other gray wolves.

Using the tree model with no admixture from TreeMix (Figure S6), we visualized the matrix of residuals (Figure S7) to determine how the estimated genetic relationship between each pair of canids fit the model. A high residual indicates that the pair does not fit the tree model and may be candidates for an admixture event. We find two candidate admixture events, the first between the Andean fox and Zhejiang wolf (Figure 2) and the second between gray wolves from Portugal and Iberia. In an ML tree allowing two admixture events, admixture from the lineage leading to the Andean fox to the lineage leading to the Zhejiang wolf is included, whereas gray wolves from Portugal and Iberia are grouped into the same cluster (Figure S8). Admixture between the outgroup Andean fox and the Zhejiang wolf supports our conclusions from the D-statistic analysis (Tables S5 and S6), in which the Zhejiang wolf possesses an ancestral component that came from a population that diverged earlier than the Jackal or Dhole did from wolves. The estimated value of the migration event in the Zhejiang individual is $12.3\% \pm 0.4\%$ ($p = 2.2 \times 10^{-308}$). In the TreeMix analysis, we used the Andean fox as an outgroup, whose distance from the included canids would result in weak phylogenetic constraints. In addition, we also used the F4-ratio test to estimate the proportion of this deep ancestry, and as it is older than the separation of the Jackal and Dhole, we used an unrooted phylogeny where the Fox is used as a proxy for the source of the deep ancestry (Figure S9). Thus, we estimate the proportion of ancestry related to the Fox, which is given by:

$$\frac{f_4(Dhole,\ Jackal,\ Coyote,\ X)}{f_4(Dhole,\ Jackal,\ Coyote,\ Andean\ Fox)},$$

where X is each gray wolf in turn.

Using this method, we found that the estimated admixture proportion of the deep ancestry for the Zhejiang wolf is $11.7\% \pm 0.5\%$, whereas all other gray wolves have an estimated admixture proportion close to zero. Similarly, in the qpGraph analysis, we estimated an admixture proportion for the deep ancestry in W7_Zhejiang of 14% (Figures S10–S14). Thus the TreeMix, F4-ratio and admixture graph analyses all support the presence of gene flow from an ancient canid population into the ancestors of the Zhejiang wolf.

Conclusion

The distribution of gray wolves in East Asia is controversial because some studies have claimed that gray wolves never existed (Callaway, 2013; Larson and Fuller, 2014) or are now extinct in SC (Lau et al., 2010), whereas others sources, especially those based on Chinese literature, have stated that they are present across all of mainland China (Wang et al., 2016b). In this study, we provide the first comparative genomic analysis of gray wolves from East Asia, focusing particularly on wolves from SC, where some believed no gray wolves were distributed (Callan et al., 2013; Larson and Fuller, 2014). Previously, Asian wolves could be divided into two populations: Tibetan gray wolves (*Canis lupus chanco*) and Chinese lowland wolves (Fan et al., 2016; Zhang et al., 2014). Here, using ancient genome-wide data, we reconstruct the phylogeny and evaluate the population structure and shared genetic drift between East Asian gray wolves to show that they form three major groups, which we call Southern China (SC), Northern Asia (NA), and Tibetan, based on their geographic distribution. Interestingly, specimens from SC gray wolves were all collected from 1963 to 1988. Our results highlight that the

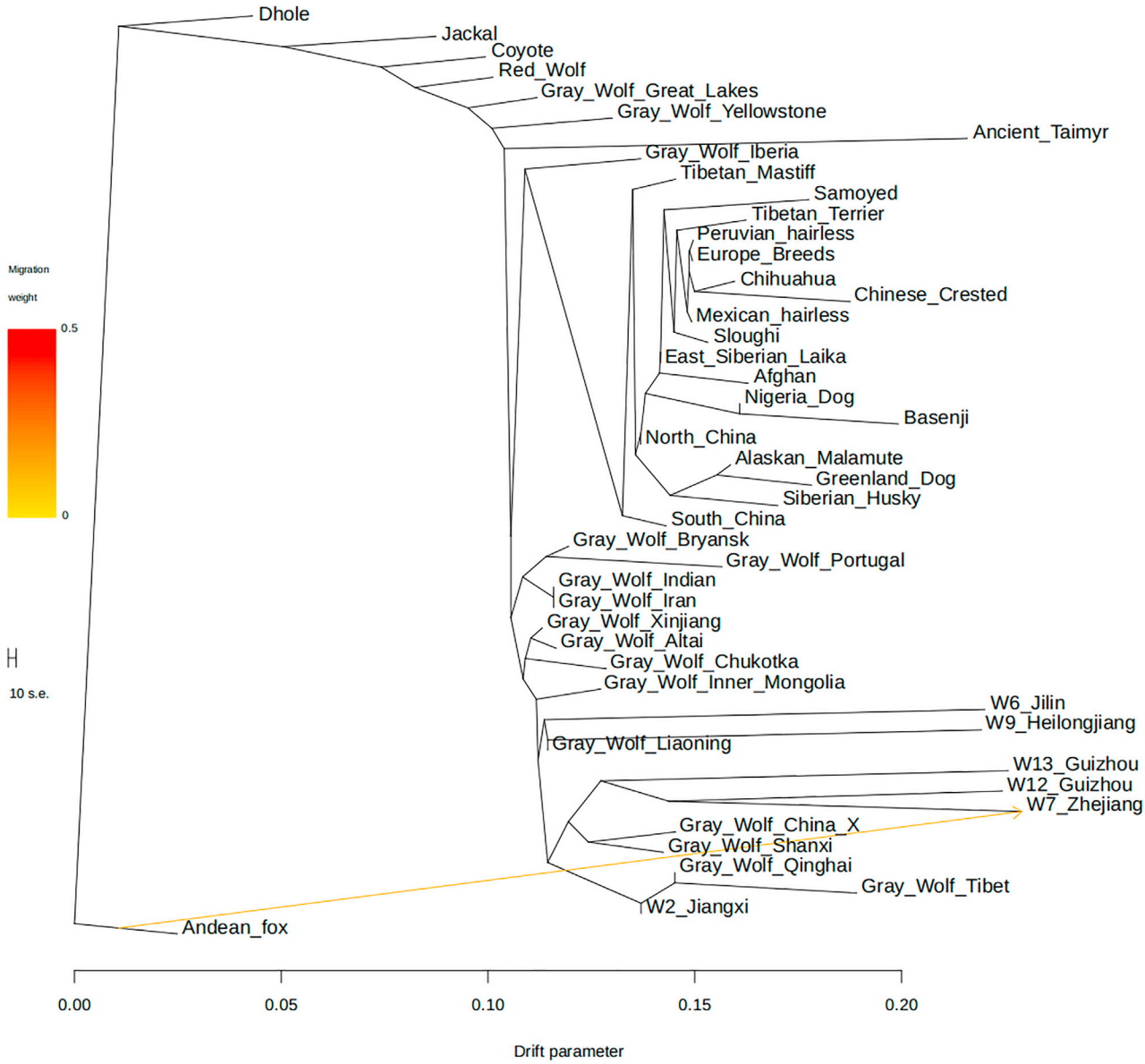

Figure 2. The Maximum Likelihood Tree Based on TreeMix with m = 1

The scale bar shows 10 times the average standard error of the entries in the sample covariance matrix. We have used the prefix "Gray_Wolf_" for highlighting gray wolves.

population in SC is endemic, and with the fast growing economic development of China, it is paramount to protect and restore their ecological habitat. Through our study, we also emphasize the value of using paleogenomic approaches to study the numerous museum specimens available (Min-Shan Ko et al., 2018; Roy et al., 1994), and we address the importance of using population genomics to determine current or future conservation efforts.

Finally, our analyses show that admixture played a large role between the different Asian wolves, and we highlight two instances here. First, we find that a wolf as far southeast as Jiangxi province shows evidence of being a mixture of Tibetan-related wolves and other wolves in China. Second, we traced an unusual admixture event in the Zhejiang wolf. In many analyses, this wolf behaved similarly to other gray wolves in China, particularly those from SC. However, tests of admixture suggest that the Zhejiang wolf shows gene flow from a canid that diverged earlier than the separation of wolves and jackals. D-statistic analysis suggests

that this may be from the Dhole, a species distributed in SC and Southeast Asia (Iyengar et al., 2005), or another canid that separated earlier than the divergence between wolves and the Dhole. Whatever the source of this ancestry, estimates of the admixture proportion from this deeply diverging population are estimated to be ~12%–14%. Our results, taken together with previous research (Gopalakrishnan et al., 2018), reveal that canids are an ideal system in which to study how gene flow can shape speciation in a genus, and highlight the need for greater study of ancient gray wolf populations.

Limitations of Study

Although our results showed support for a SC gray wolf population and strong evidence for interspecific gene flow to the W7_Zhejiang wolf, the source of the interspecific gene flow into W7_Zhejiang is unclear. The availability of few specimens makes sampling in appropriate regions difficult, and where specimens are available, obtaining high coverage genomic data is not easy owing to natural degradation processes and loss of genetic material from museum storage methods. More samples are needed in future studies to further understand the admixture dynamics in canids.

METHODS

All methods can be found in the accompanying Transparent Methods supplemental file.

DATA AND CODE AVAILABILITY

The accession number for the sequence data of six gray wolf genomes in this paper is GSA: PRJCA001135 and the SRA: PRJEB34110. The SNP set is available on the iDog database (http://bigd.big.ac.cn/idog/).

SUPPLEMENTAL INFORMATION

Supplemental Information can be found online at https://doi.org/10.1016/j.isci.2019.09.008.

ACKNOWLEDGMENTS

We thank Jun Chen and Gexia Qiao from the National Zoological Museum of China, Beijing, China, and Weiwei Li and Song Li from the Kunming Natural History Museum of Zoology, Yunnan, China, for helping to collect wolf skin specimens. We thank the BIG Data Center at the Beijing Institute of Genomics, Chinese Academy of Sciences (CAS), for use of their high-performance computing platform. This work was supported by the Strategic Priority Research Program (B) (XDB13000000, XDB26000000) of the CAS, National Natural Science Foundation of China (91731304, 91731303, 41672021, and 41630102). P.S. was supported by the Francis Crick Institute, which receives its core funding from Cancer Research UK (FC001595), the UK Medical Research Council (FC001595), and the Wellcome Trust (FC001595). Q.F. is supported by CAS (XDA19050102, QYZDB-SSW-DQC003), and the Howard Hughes Medical Institute (grant number 55008731). G.-D.W. is supported by the Youth Innovation Promotion Association, CAS, and the CAS international collaborating grant proposal (152453KYSB20150002). This work was supported by the Animal Branch of the Germplasm Bank of Wild Species, CAS (the Large Research Infrastructure Funding).

AUTHOR CONTRIBUTIONS

Y.-P.Z. and Q.F. designed research. G.-D.W. and Q.F. managed the project. L.W. collected samples. P.C., F.L., M.Z., and X.F. performed DNA experiments. Q.F., X.F., M.A.Y., and P.S. did the data processing. Q.F., G.-D.W., M.Z., X.W., M.A.Y., and H.L. analyzed the data. G.-D.W., M.A.Y., Q.F., and Y.-P.Z. wrote the manuscript.

DECLARATION OF INTERESTS

The authors declare no competing interests.

Received: February 26, 2019
Revised: June 21, 2019
Accepted: September 5, 2019
Published: October 25, 2019

REFERENCES

Auton, A., Li, Y.R., Kidd, J., Oliveira, K., Nadel, J., Holloway, J.K., Hayward, J.J., Cohen, P.E., Greally, J.M., Wang, J., et al. (2013). Genetic recombination is targeted towards gene promoter regions in dogs. PLoS Genet. *9*, e1003984.

Botigué, L.R., Song, S., Scheu, A., Gopalan, S., Pendleton, A.L., Oetjens, M., Taravella, A.M., Seregély, T., Zeeb-Lanz, A., Arbogast, R.-M., et al. (2017). Ancient European dog genomes reveal continuity since the Early Neolithic. Nat. Commun. *8*, 16082.

Briggs, A.W., Stenzel, U., Johnson, P.L., Green, R.E., Kelso, J., Prufer, K., Meyer, M., Krause, J., Ronan, M.T., Lachmann, M., et al. (2007). Patterns of damage in genomic DNA sequences from a Neandertal. Proc. Natl. Acad. Sci. U S A *104*, 14616–14621.

Callan, R., Nibbelink, N.P., Rooney, T.P., Wiedenhoeft, J.E., and Wydeven, A.P. (2013). Recolonizing wolves trigger a trophic cascade in Wisconsin (USA). J. Ecol. *101*, 837–845.

Callaway, E. (2013). Dog genetics spur scientific spat. Nature *498*, 282–283.

Carmichael, L.E., Nagy, J.A., Larter, N.C., and Strobeck, C. (2001). Prey specialization may influence patterns of gene flow in wolves of the Canadian Northwest. Mol. Ecol. *10*, 2787–2798.

Dabney, J., Knapp, M., Glocke, I., Gansauge, M.T., Weihmann, A., Nickel, B., Valdiosera, C., Garcia, N., Paabo, S., Arsuaga, J.L., et al. (2013). Complete mitochondrial genome sequence of a Middle Pleistocene cave bear reconstructed from ultrashort DNA fragments. Proc. Natl. Acad. Sci. U S A *110*, 15758–15763.

Decker, B., Davis, B.W., Rimbault, M., Long, A.H., Karlins, E., Jagannathan, V., Reiman, R., Parker, H.G., Drogemuller, C., Corneveaux, J.J., et al. (2015). Comparison against 186 canid whole-genome sequences reveals survival strategies of an ancient clonally transmissible canine tumor. Genome Res. *25*, 1646–1655.

DePristo, M.A., Banks, E., Poplin, R., Garimella, K.V., Maguire, J.R., Hartl, C., Philippakis, A.A., del Angel, G., Rivas, M.A., Hanna, M., et al. (2011). A framework for variation discovery and genotyping using next-generation DNA sequencing data. Nat. Genet. *43*, 491–498.

Fan, Z., Silva, P., Gronau, I., Wang, S., Armero, A.S., Schweizer, R.M., Ramirez, O., Pollinger, J., Galaverni, M., Ortega Del-Vecchyo, D., et al. (2016). Worldwide patterns of genomic variation and admixture in gray wolves. Genome Res. *26*, 163–173.

Frantz, L.A., Mullin, V.E., Pionnier-Capitan, M., Lebrasseur, O., Ollivier, M., Perri, A., Linderholm, A., Mattiangeli, V., Teasdale, M.D., Dimopoulos, E.A., et al. (2016). Genomic and archaeological evidence suggest a dual origin of domestic dogs. Science *352*, 1228–1231.

Freedman, A.H., Gronau, I., Schweizer, R.M., Ortega-Del Vecchyo, D., Han, E., Silva, P.M., Galaverni, M., Fan, Z., Marx, P., Lorente-Galdos, B., et al. (2014). Genome sequencing highlights the dynamic early history of dogs. PLoS Genet. *10*, e1004016.

Geffen, E., Anderson, M.J., and Wayne, R.K. (2004). Climate and habitat barriers to dispersal in the highly mobile grey wolf. Mol. Ecol. *13*, 2481–2490.

Gopalakrishnan, S., Sinding, M.S., Ramos-Madrigal, J., Niemann, J., Samaniego Castruita, J.A., Vieira, F.G., Caroe, C., Montero, M.M., Kuderna, L., Serres, A., et al. (2018). Interspecific gene flow shaped the evolution of the genus canis. Curr. Biol. *28*, 3441–3449.e5.

Iyengar, A., Babu, V.N., Hedges, S., Venkataraman, A.B., Maclean, N., and Morin, P.A. (2005). Phylogeography, genetic structure, and diversity in the dhole (*Cuon alpinus*). Mol. Ecol. *14*, 2281–2297.

Kircher, M., Sawyer, S., and Meyer, M. (2012). Double indexing overcomes inaccuracies in multiplex sequencing on the Illumina platform. Nucleic Acids Res. *40*, e3.

Larson, G., and Fuller, D.Q. (2014). The evolution of animal domestication. Annu. Rev. Ecol. Evol. Syst. *45*, 115–136.

Lau, M.W.N., Fellowes, J.R., and Chan, B.P.L. (2010). Carnivores (Mammalia: Carnivora) in South China: a status review with notes on the commercial trade. Mamm. Rev. *40*, 247–292.

Lindblad-Toh, K., Wade, C.M., Mikkelsen, T.S., Karlsson, E.K., Jaffe, D.B., Kamal, M., Clamp, M., Chang, J.L., Kulbokas, E.J., 3rd, Zody, M.C., et al. (2005). Genome sequence, comparative analysis and haplotype structure of the domestic dog. Nature *438*, 803–819.

Liu, Y.H., Wang, L., Xu, T., Guo, X., Li, Y., Yin, T.T., Yang, H.C., Hu, Y., Adeola, A.C., Sanke, O.J., et al. (2018). Whole-genome sequencing of african dogs provides insights into adaptations against tropical parasites. Mol. Biol. Evol. *35*, 287–298.

Loog, L., Thalmann, O., Sinding, M.-H.S., Schuenemann, V.J., Perri, A., Germonpre, M., Bocherens, H., Witt, K.E., Samaniego Castruita, J.A., Velasco, M.S., et al. (2018). Modern wolves trace their origin to a late Pleistocene expansion from Beringia. bioRxiv. https://doi.org/10.1101/370122.

Macdonald, D.W., and Sillero-Zubiri, C. (2004). Biology and Conservation of Wild Canids (Oxford University Press).

Marsden, C.D., Ortega-Del Vecchyo, D., O'Brien, D.P., Taylor, J.F., Ramirez, O., Vila, C., Marques-Bonet, T., Schnabel, R.D., Wayne, R.K., and Lohmueller, K.E. (2016). Bottlenecks and selective sweeps during domestication have increased deleterious genetic variation in dogs. Proc. Natl. Acad. Sci. U S A *113*, 152–157.

Meyer, M., and Kircher, M. (2010). Illumina sequencing library preparation for highly multiplexed target capture and sequencing. Cold Spring Harb Protoc. *2010*, https://doi.org/10.1101/pdb.prot5448.

Min-Shan Ko, A., Zhang, Y., Yang, M.A., Hu, Y., Cao, P., Feng, X., Zhang, L., Wei, F., and Fu, Q. (2018). Mitochondrial genome of a 22,000-year-old giant panda from southern China reveals a new panda lineage. Curr. Biol. *28*, R693–R694.

Monzon, J., Kays, R., and Dykhuizen, D.E. (2014). Assessment of coyote-wolf-dog admixture using ancestry-informative diagnostic SNPs. Mol. Ecol. *23*, 182–197.

Patterson, N., Moorjani, P., Luo, Y., Mallick, S., Rohland, N., Zhan, Y., Genschoreck, T., Webster, T., and Reich, D. (2012). Ancient admixture in human history. Genetics *192*, 1065–1093.

Patterson, N., Price, A.L., and Reich, D. (2006). Population structure and eigenanalysis. PLoS Genet. *2*, e190.

Pickrell, J.K., and Pritchard, J.K. (2012). Inference of population splits and mixtures from genome-wide allele frequency data. PLoS Genet. *8*, e1002967.

Pilot, M., Greco, C., vonHoldt, B.M., Jedrzejewska, B., Randi, E., Jedrzejewski, W., Sidorovich, V.E., Ostrander, E.A., and Wayne, R.K. (2014). Genome-wide signatures of population bottlenecks and diversifying selection in European wolves. Heredity (Edinb.) *112*, 428–442.

Pilot, M., Jedrzejewski, W., Branicki, W., Sidorovich, V.E., Jedrzejewska, B., Stachura, K., and Funk, S.M. (2006). Ecological factors influence population genetic structure of European grey wolves. Mol. Ecol. *15*, 4533–4553.

Pocock, R.I. (1941). The Fauna of British India Including Ceylon and Burma. In Mammalia, Vol. II. Carnivora, R.B.S. Sewel, ed. (Taylor and Francis), p. 504.

Raghavan, M., Skoglund, P., Graf, K.E., Metspalu, M., Albrechtsen, A., Moltke, I., Rasmussen, S., Stafford, T.W., Jr., Orlando, L., Metspalu, E., et al. (2014). Upper Palaeolithic Siberian genome reveals dual ancestry of Native Americans. Nature *505*, 87–91.

Roy, M.S., Girman, D.J., Taylor, A.C., and Wayne, R.K. (1994). The use of museum specimens to reconstruct the genetic-variability and relationships of extinct populations. Experientia *50*, 551–557.

Shannon, L.M., Boyko, R.H., Castelhano, M., Corey, E., Hayward, J.J., McLean, C., White, M.E., Abi Said, M., Anita, B.A., Bondjengo, N.I., et al. (2015). Genetic structure in village dogs reveals a Central Asian domestication origin. Proc. Natl. Acad. Sci. U S A *112*, 13639–13644.

Skoglund, P., Ersmark, E., Palkopoulou, E., and Dalen, L. (2015). Ancient wolf genome reveals an early divergence of domestic dog ancestors and admixture into high-latitude breeds. Curr. Biol. *25*, 1515–1519.

Smith, A.T., and Xie, Y. (2014). A Guide to the Mammals of China (Princeton University Press).

Tang, B., Zhou, Q., Dong, L., Li, W., Zhang, X., Lan, L., Zhai, S., Xiao, J., Zhang, Z., Bao, Y., et al. (2019). iDog: an integrated resource for domestic dogs and wild canids. Nucleic Acids Res. *47*, D793–D800.

Thalmann, O., Shapiro, B., Cui, P., Schuenemann, V.J., Sawyer, S.K., Greenfield, D.L., Germonpre, M.B., Sablin, M.V., Lopez-Giraldez, F., Domingo-Roura, X., et al. (2013). Complete mitochondrial

genomes of ancient canids suggest a European origin of domestic dogs. Science *342*, 871–874.

vonHoldt, B.M., Cahill, J.A., Fan, Z., Gronau, I., Robinson, J., Pollinger, J.P., Shapiro, B., Wall, J., and Wayne, R.K. (2016). Whole-genome sequence analysis shows that two endemic species of North American wolf are admixtures of the coyote and gray wolf. Sci. Adv. *2*, e1501714.

vonHoldt, B.M., Pollinger, J.P., Earl, D.A., Knowles, J.C., Boyko, A.R., Parker, H., Geffen, E., Pilot, M., Jedrzejewski, W., Jedrzejewska, B., et al. (2011). A genome-wide perspective on the evolutionary history of enigmatic wolf-like canids. Genome Res. *21*, 1294–1305.

Vonholdt, B.M., Pollinger, J.P., Lohmueller, K.E., Han, E., Parker, H.G., Quignon, P., Degenhardt, J.D., Boyko, A.R., Earl, D.A., Auton, A., et al. (2010). Genome-wide SNP and haplotype analyses reveal a rich history underlying dog domestication. Nature *464*, 898–902.

Wang, G.D., Shao, X.J., Bai, B., Wang, J.L., Wang, X.B., Cao, X., Liu, Y.H., Wang, X., Yin, T.T., Zhang, S.J., et al. (2019a). Structural variation during dog domestication: insights from gray wolf and dhole genomes. Natl. Sci. Rev. *6*, 110–122.

Wang, G.D., Zhai, W., Yang, H.C., Wang, L., Zhong, L., Liu, Y.H., Fan, R.X., Yin, T.T., Zhu, C.L., Poyarkov, A.D., et al. (2016a). Out of southern East Asia: the natural history of domestic dogs across the world. Cell Res. *26*, 21–33.

Wang, G.D., Zhai, W.W., Yang, H.C., Fan, R.X., Cao, X., Zhong, L., Wang, L., Liu, F., Wu, H., Cheng, L.G., et al. (2013). The genomics of selection in dogs and the parallel evolution between dogs and humans. Nat. Commun. *4*, 1860.

Wang, L., Ma, Y.P., Zhou, Q.J., Zhang, Y.P., Savolaimen, P., and Wang, G.D. (2016b). The geographical distribution of grey wolves (*Canis lupus*) in China: a systematic review. Zool. Res. *37*, 315–326.

Wang, X., Zhou, B.W., Yang, M.A., Yin, T.T., Chen, F.L., Ommeh, S.C., Esmailizadeh, A., Turner, M.M., Poyarkov, A.D., Savolainen, P., et al. (2019b). Canine transmissible venereal tumor genome reveals ancient introgression from coyotes to pre-contact dogs in North America. Cell Res. *29*, 592–595.

Wayne, R.K., Geffen, E., Girman, D.J., Koepfli, K.P., Lau, L.M., and Marshall, C.R. (1997). Molecular systematics of the Canidae. Syst. Biol. *46*, 622–653.

Wayne, R.K., Lehman, N., Allard, M.W., and Honeycutt, R.L. (1992). Mitochondrial-DNA variability of the gray wolf - genetic consequences of population decline and habitat fragmentation. Conserv. Biol. *6*, 559–569.

Wilson, D.E., and Reeder, D.M. (2005). Mammal Species of the World: A Taxonomic and Geographic Reference, Third Edition (Johns Hopkins University Press).

Young, S.P., and Goldman, E.A.; American Wildlife, F. (1944). The Wolves of North America. Part-II. Classification of Wolves, First Edition (The American Wildlife Institute).

Zhang, W., Fan, Z., Han, E., Hou, R., Zhang, L., Galaverni, M., Huang, J., Liu, H., Silva, P., Li, P., et al. (2014). Hypoxia adaptations in the grey wolf (*Canis lupus chanco*) from Qinghai-Tibet Plateau. PLoS Genet. *10*, e1004466.

ISCI, Volume *20*

Supplemental Information

Genomic Approaches Reveal an Endemic Subpopulation of Gray Wolves in Southern China

Guo-Dong Wang, Ming Zhang, Xuan Wang, Melinda A. Yang, Peng Cao, Feng Liu, Heng Lu, Xiaotian Feng, Pontus Skoglund, Lu Wang, Qiaomei Fu, and Ya-Ping Zhang

Supplemental Information

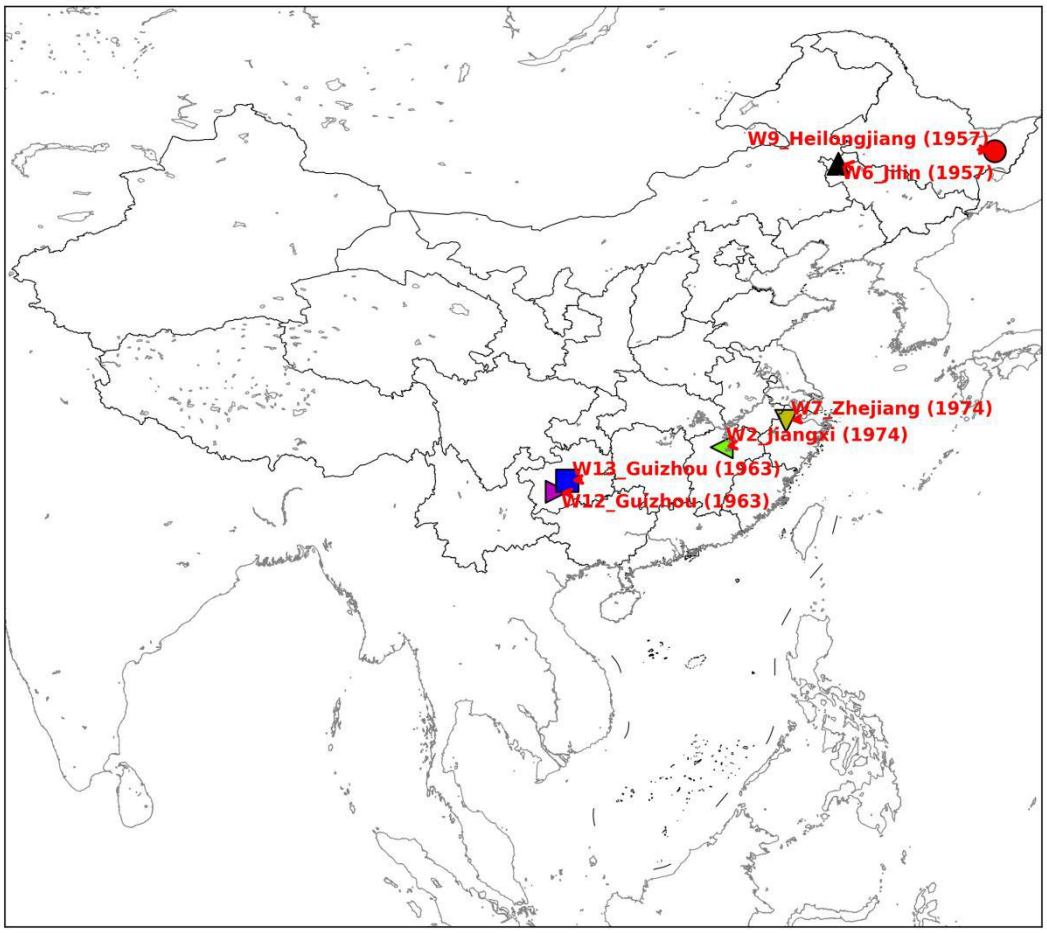

Figure S1. Geographical origin of six museum wolf skin specimens in China, two samples from Guizhou. The collection year is indicated in parantheses. Related to Figure 1.

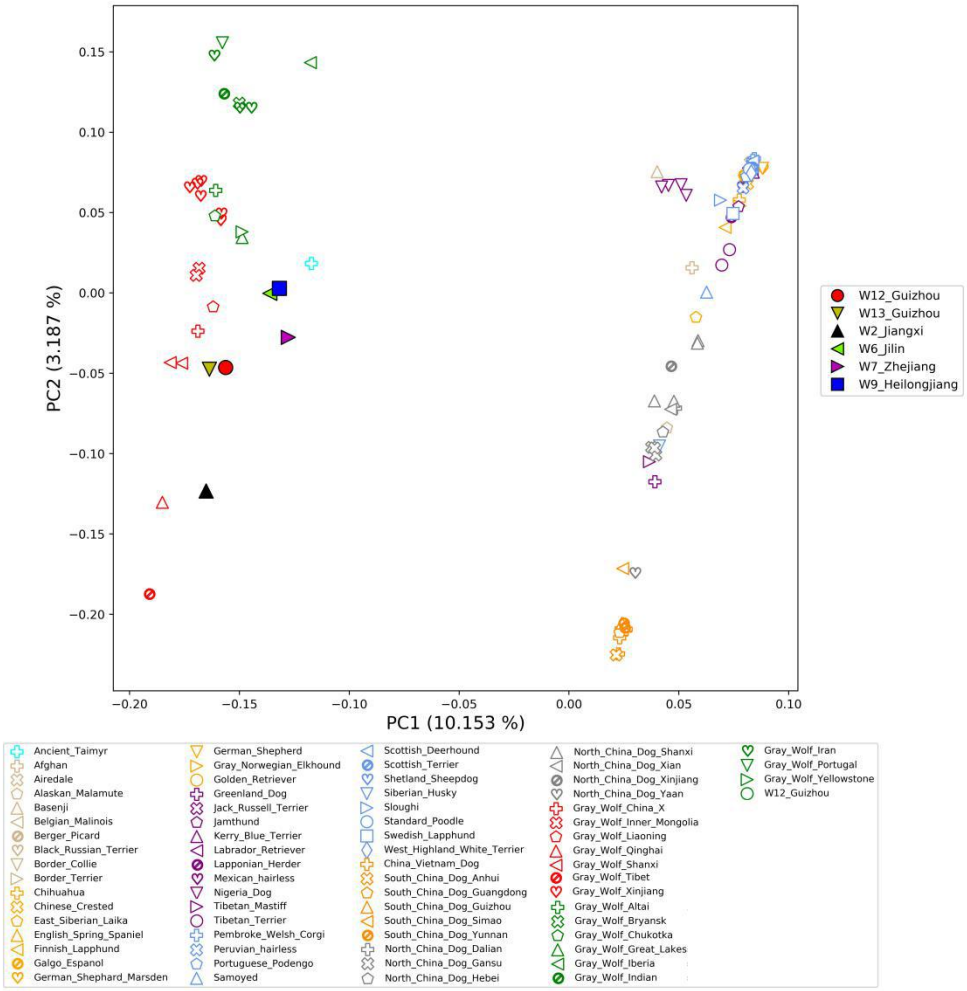

Figure S2. PCA analysis with wolf and dog populations. We have used the prefix "Gray_Wolf_" for highlighting specimens of gray wolves. Related to Figure 1.

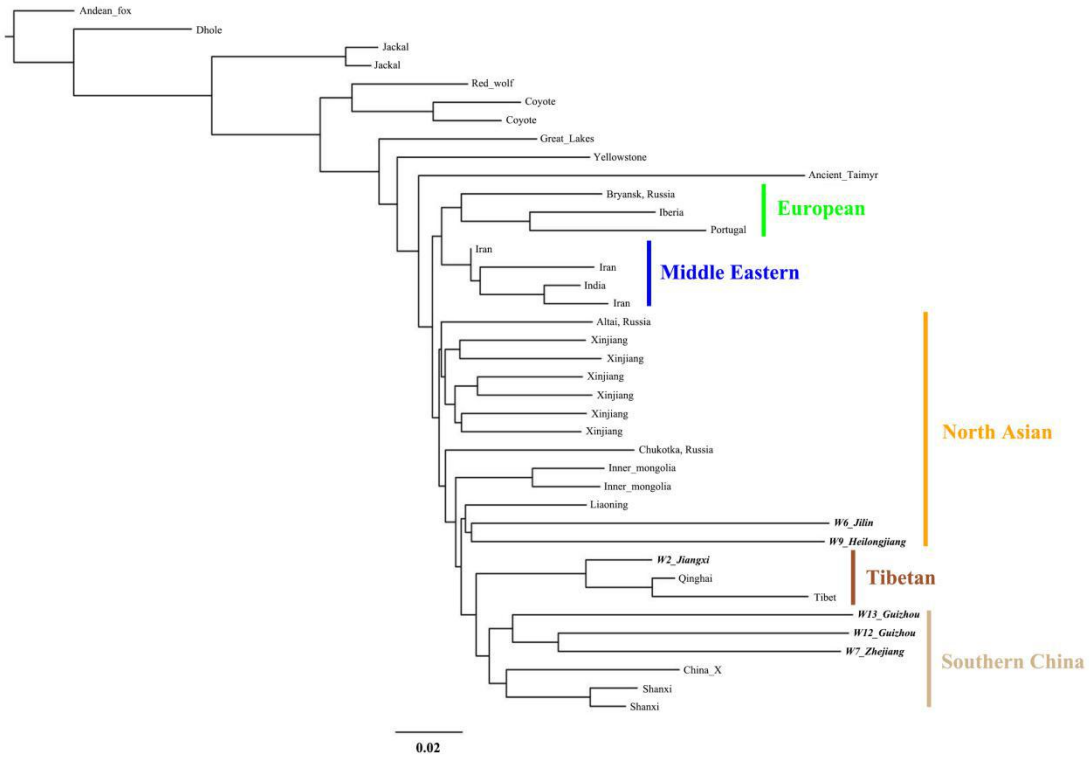

Figure S3. Neighbor-Joining tree including 39 canids without dogs. The Andean fox is the outgroup. The newly sequenced individuals are marked in bold and are italicized. Related to Figure 1.

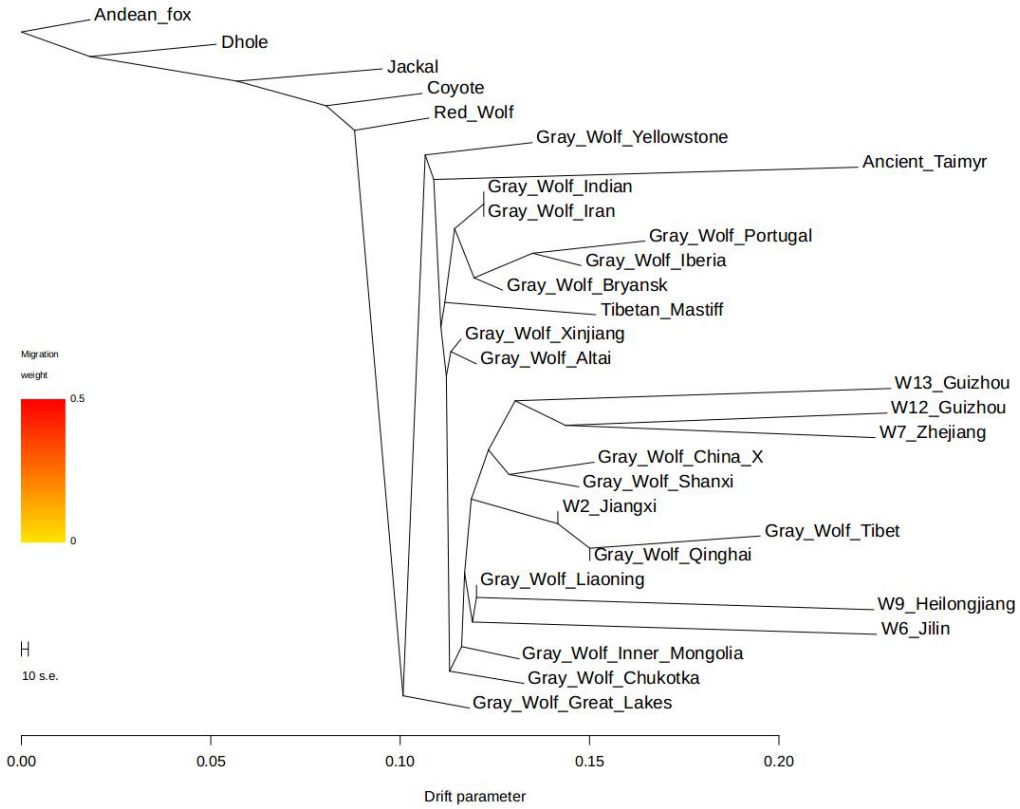

Figure S4. The maximum-likelihood tree based on TreeMix using 39 canids without dogs and m=0. The scale bar shows ten times the average standard error of the entries in the sample covariance matrix. Related to Figure 2.

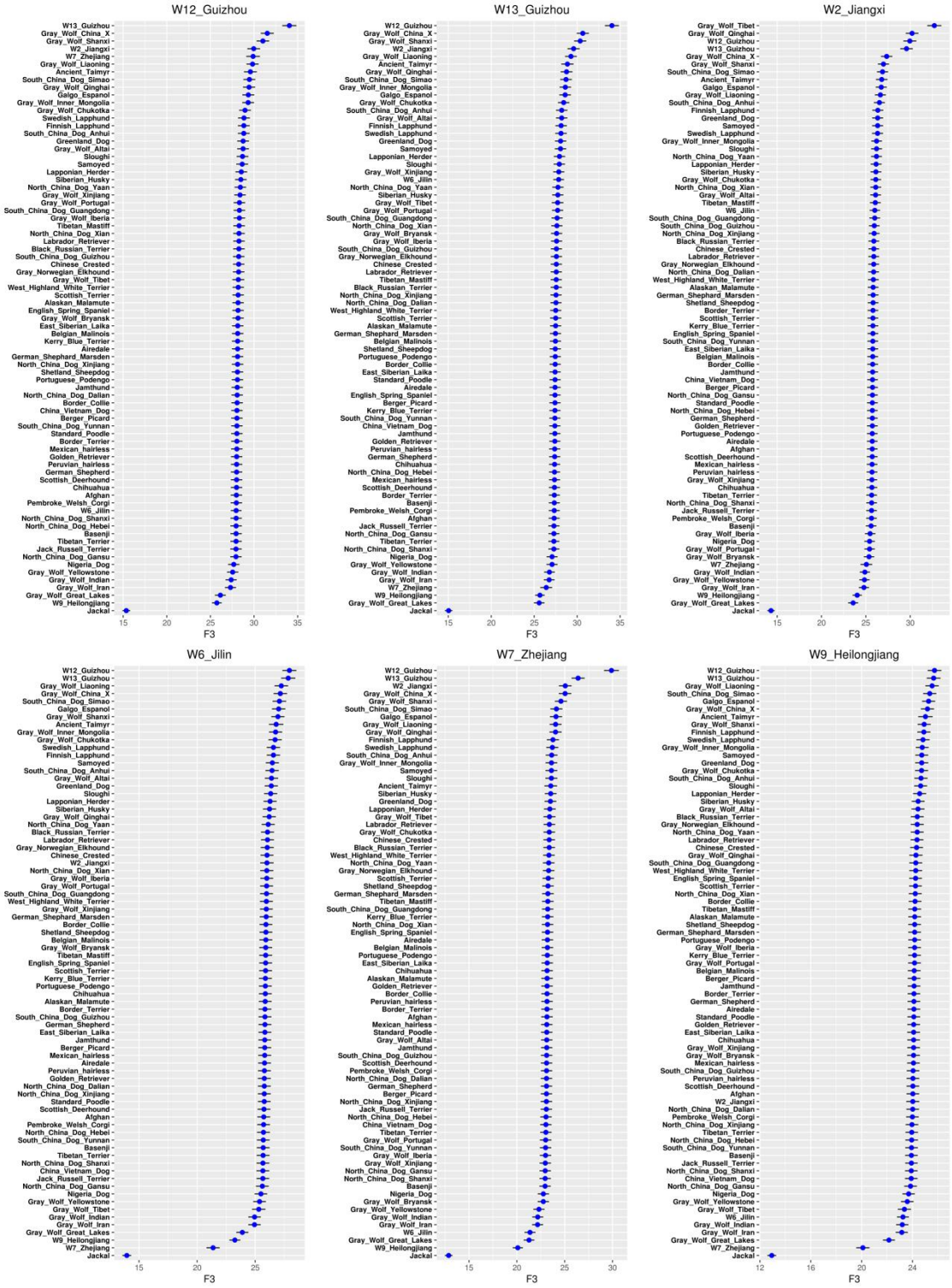

Figure S5. f3(Dhole; X, Y), where X is one of the six newly sequenced wolves and Y are other canids. We have used the prefix "Gray_Wolf_" for highlighting specimens of gray wolves. Related to Figure 1.

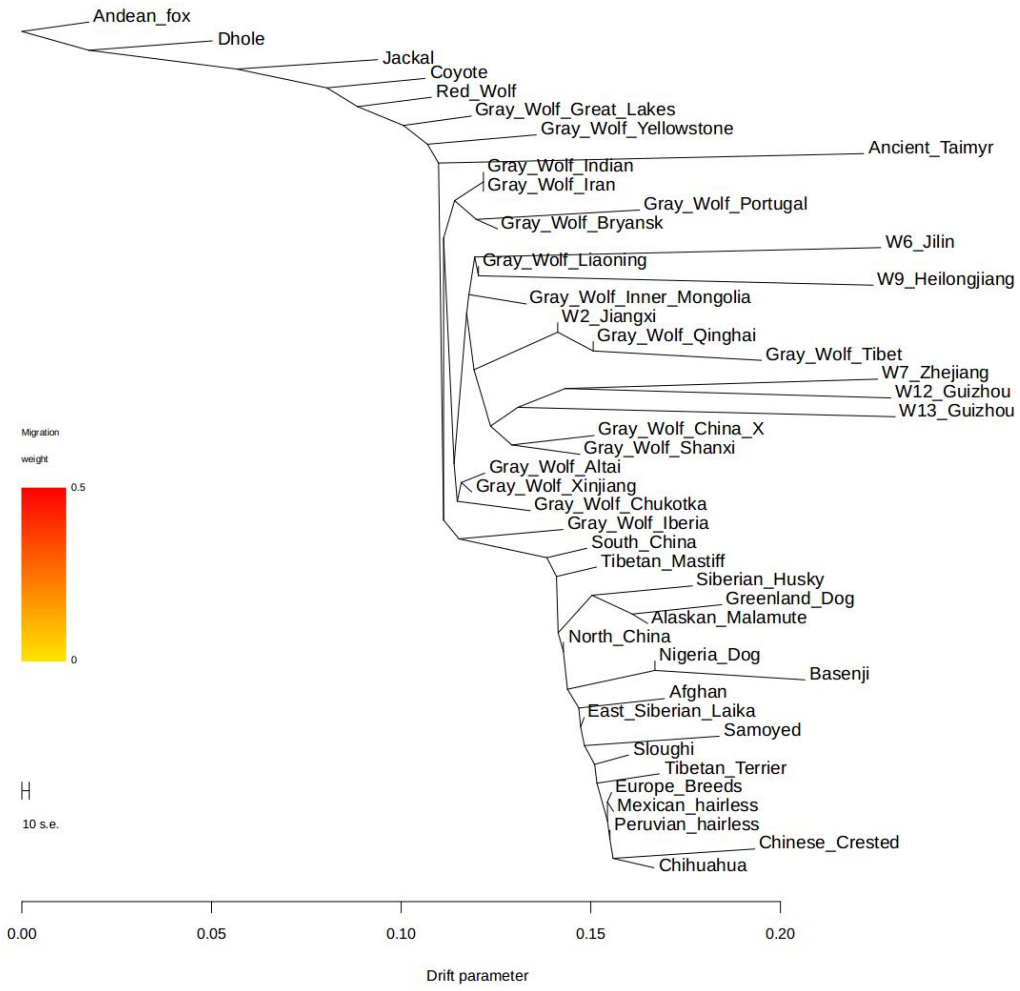

Figure S6. The maximum-likelihood tree based on TreeMix with m=0 for all canids. The scale bar shows ten times the average standard error of the entries in the sample covariance matrix. We have used the prefix "Gray_Wolf_" for highlighting specimens of gray wolves. Related to Figure 2.

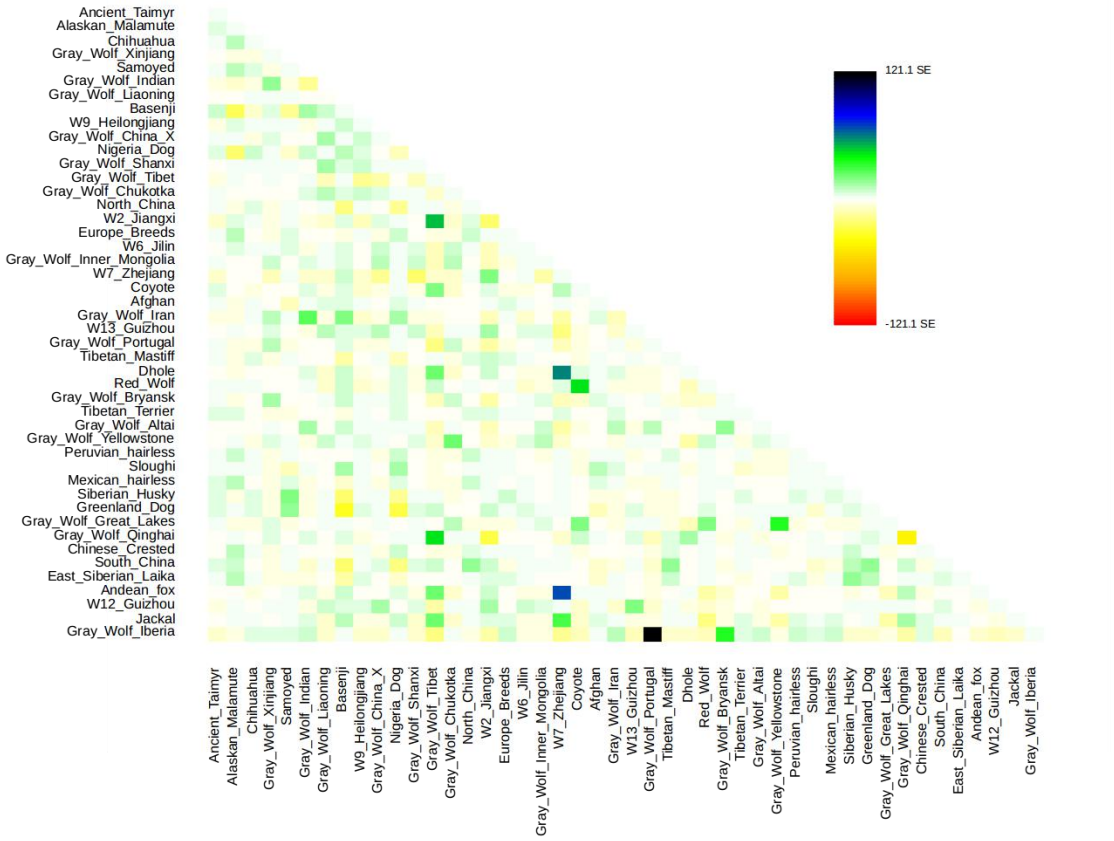

Figure S7. The residual fit from the maximum likelihood tree in Figure S6. This is determined by dividing the residual covariance between each pair of populations by the average standard error across all pairs. Colors are described in the palette on the right. Residuals above zero represent populations that are more closely related to each other in the data than in the best-fit tree, and thus are candidates for admixture events. We have used the prefix "Gray_Wolf_" for highlighting specimens of gray wolves. Related to Figure 2.

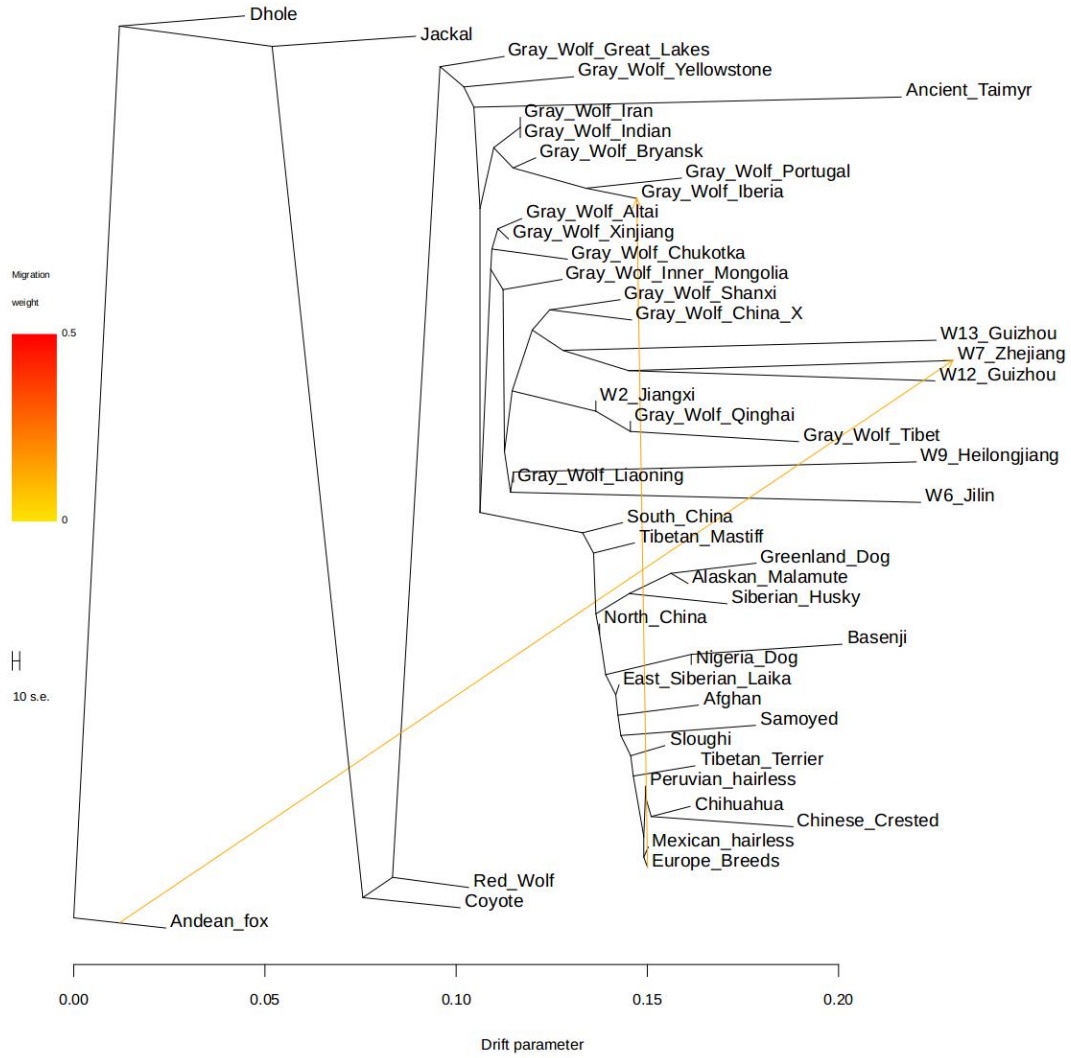

Figure S8. The maximum-likelihood tree based on TreeMix with m=2. The scale bar shows ten times the average standard error of the entries in the sample covariance matrix. We have used the prefix "Gray_Wolf_" for highlighting specimens of gray wolves. Related to Figure 2.

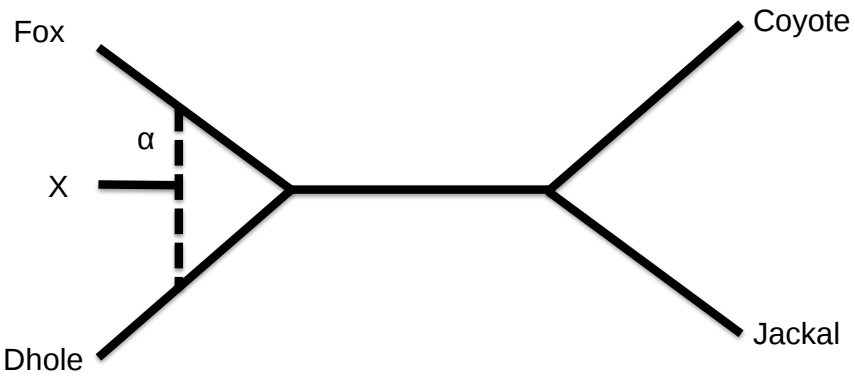

Figure S9. Unrooted tree used to estimate the archaic admixture proportion in the Zhejiang wolf. Related to Figure 2.

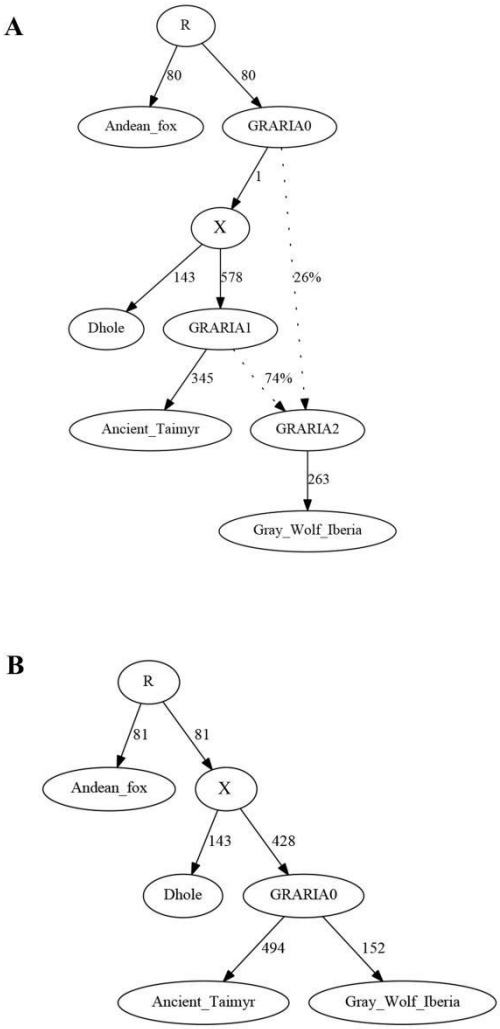

Figure S10. Basal Admixture Graph model with Gray_Wolf_Iberia added. Related to Figure 2.

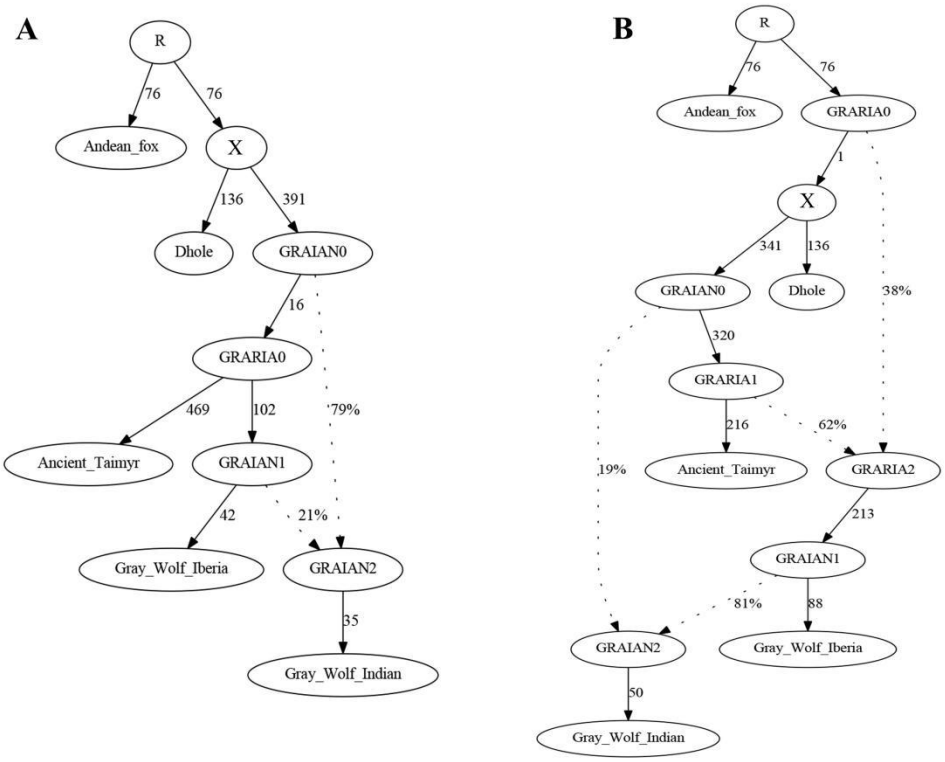

Figure S11. Adding Gray_Wolf_Indian to the graphs from Figure S10. Related to Figure 2.

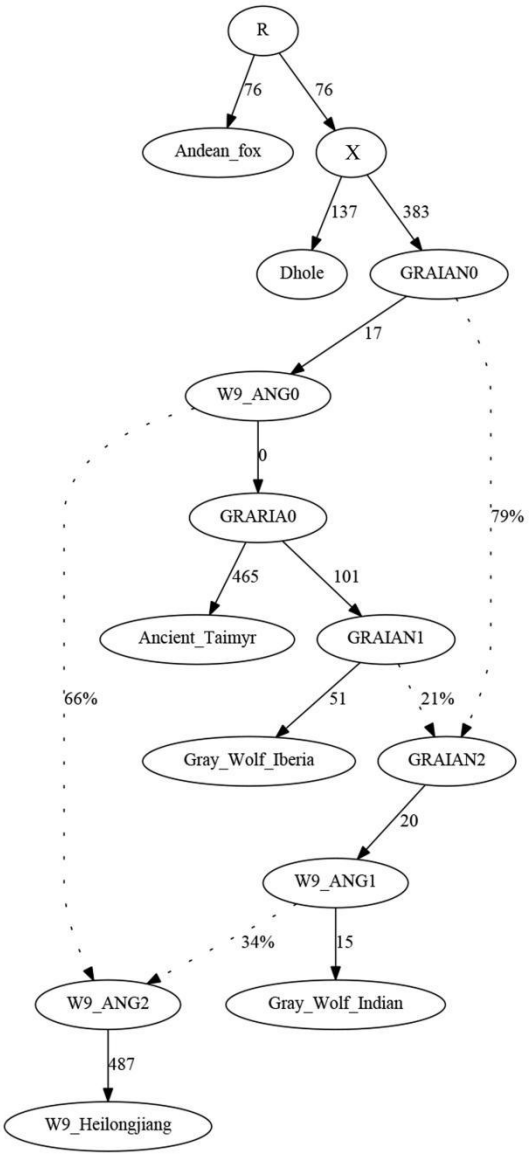

Figure S12. Adding W9_Heilongjiang to the graphs from Figure S11. Related to Figure 2.

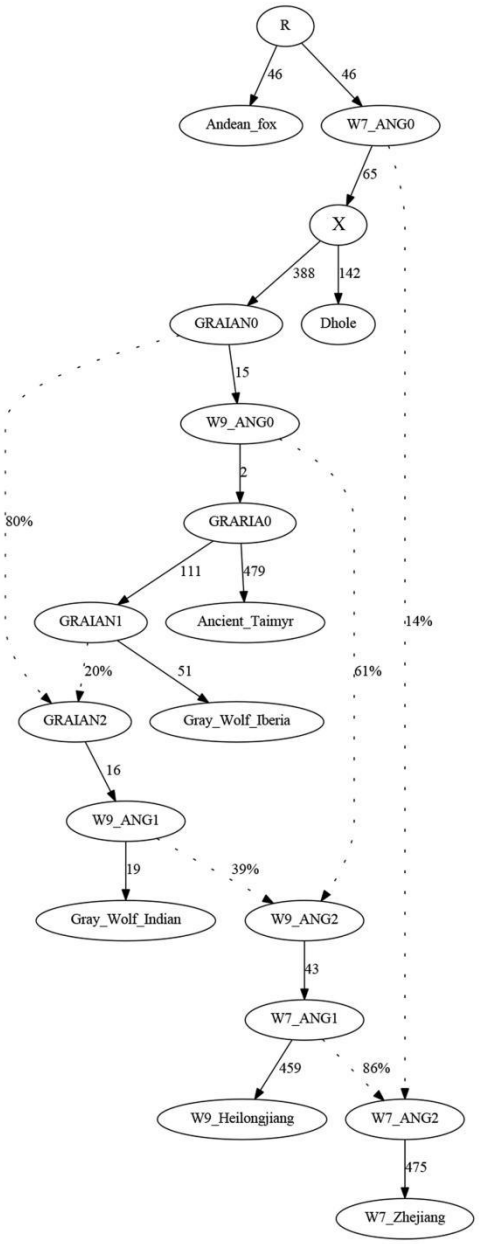

Figure S13. Adding W7_Zhejiang to the graphs from Figure S12. Related to Figure 2.

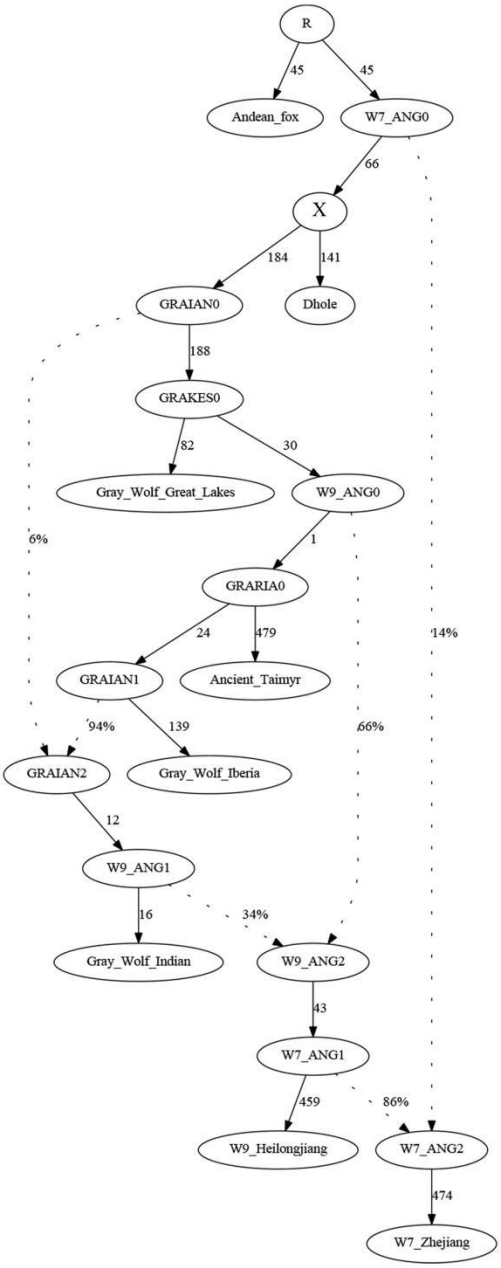

Figure S14. Adding Gray_Wolf_Great_Lakes to the graphs from Figure S13. Related to Figure 2.

Table S1. Sequencing metrics on the libraries of the samples. Related to Table 1.

Sample_ID	Lib_ID	Raw	Merged	&L30	Mapped	%Mapped	Unique	Average Length
W12_Guizhou	L4705	285343617	282720996	279349969	193639299	69	87020138	66
W12_Guizhou	L4706	122888988	121920909	120203042	81036195	67	37300930	66
W12_Guizhou	L4723	99422832	98301650	95950384	66689079	70	27296673	60
W12_Guizhou	L4724	129941007	128741838	125878134	86419489	69	35693699	60
W12_Guizhou	L4721	458823905	457178101	448236865	354599384	79	172415148	75
W12_Guizhou	L1236	220782482	214658250	212167619	172702204	81	83601122	82
W13_Guizhou	L4715	174435249	170656674	168612632	143289506	85	67178876	71
W13_Guizhou	L4733	100006948	97480812	96184443	79766884	83	37206113	74
W13_Guizhou	L4716	139660264	136843871	135476042	94368328	70	41458135	75
W13_Guizhou	L4734	72759420	71413179	70557705	48841322	69	20183735	72
W13_Guizhou	L1237	376669471	358779675	356919462	259792144	73	138338276	94
W2_Jiangxi	L4717	57032184	56165346	55929745	49470031	88	25470196	81
W2_Jiangxi	L4718	108657013	107230625	106675141	95573663	90	49006998	78
W2_Jiangxi	L4735	84038690	82911815	82368601	73430883	89	34211885	74
W2_Jiangxi	L4736	904760479	897952829	896171857	792391018	88	457142173	92
W2_Jiangxi	L1228	614619758	568519001	567900196	519132756	91	335201526	126
W6_Jilin	L4707	127681136	126097468	118289082	90384661	76	26902055	48
W6_Jilin	L4708	125430513	123589141	116027856	87251813	75	25879613	49
W6_Jilin	L4725	58051880	57192340	49981995	32368357	65	10635232	43
W6_Jilin	L4726	77378791	76219741	65107619	47902350	74	15267977	42
W6_Jilin	L1232	389136153	325919319	315703233	246562564	78	11324756	58
W7_Zhejiang	L4709	39112069	38593429	35402488	1843676	5	732974	57
W7_Zhejiang	L4710	35581720	35083335	32713276	1193424	4	395721	56
W7_Zhejiang	L4711	39015421	38438945	35639593	1833027	5	705431	64
W7_Zhejiang	L4712	39853260	39242507	36562343	2739467	7	1008169	63
W7_Zhejiang	L4727	39610530	39030578	32984973	2129260	6	796738	47
W7_Zhejiang	L4728	35207785	34640731	29296827	1317589	4	404382	46
W7_Zhejiang	L4729	44741369	44125280	37579861	2065001	5	683061	55
W7_Zhejiang	L4730	35964348	35467842	30198475	2576745	9	810242	54
W7_Zhejiang	L1233	216672870	196311964	188328108	8194354	4	324626	89
W9_Heilongjiang	L4713	60306027	59823823	56491103	48351903	86	17888738	51
W9_Heilongjiang	L4714	48275546	47733287	45095180	35539238	79	13910738	51
W9_Heilongjiang	L4731	78659917	78002396	69178887	58004190	84	20595472	44
W9_Heilongjiang	L4732	67266981	66511206	60235429	47951316	80	18366379	45
W9_Heilongjiang	L1234	146878870	129755983	125676741	53058660	42	1949475	71

Table S2. Genome information from public databases. Related to Table 1.

Species	Location	ID	Data sources
Fox	Andean	Andean_fox	Adam Auton et al., 2013, Plos Genetics
Dhole	Beijing Zoo	RUFZCHN00001	Guo-Dong Wang et al., 2018, National Science Review
Jackals	Krasnodar, Russia	AUR008537	Xuan Wang et al., 2019, Cell Research
	Krasnodar, Russia	AUR008538	Xuan Wang et al., 2019, Cell Research
Coyotes	Monterey area, Canada	LAT007000	Xuan Wang et al., 2019, Cell Research
	California, US	SAMN02921301	Bridgett M. vonHoldt et al., 2016, Science Advances
Red wolf	USA	SAMN02921317	Bridgett M. vonHoldt et al., 2016, Science Advances
Ancient wolf	Taimyr, Russia	Taimyr	Pontus Skoglund et al., 2015, Current Biology
Gray wolves	Great Lakes, USA	gwglw_RKW2455	Bridgett M. vonHoldt et al., 2016, Science Advances
	Yellowstone, USA	gwynp_RWK1547	Bridgett M. vonHoldt et al., 2016, Science Advances
	Iran	LUP004103	Xuan Wang et al., 2019, Cell Research
	Iran	LUP004107	Xuan Wang et al., 2019, Cell Research
	Iran	gwirw_RKW3073	Clare D. Marsden et al., 2016, PNAS
	India	SAMN02921311	Bridgett M. vonHoldt et al., 2016, Science Advances
	Bryansk, Russia	LUPWRUS00003	Guo-Dong Wang et al., 2013, Nature Communications
	Iberia	gwibe_XXWIB98	Laura R. Botigue et al., 2017, Nature Communications
	Portugal	gwprt_LOBO423	Clare D. Marsden et al., 2016, PNAS
	Shanxi, China	LUPZCHN00005	Guo-Dong Wang et al., 2016, Cell Research
	Shanxi, China	LUPZCHN00006	Guo-Dong Wang et al., 2016, Cell Research
	San Diego Zoo (from China)	gwcwz_RKW3916	Adam H. Freedman et al., 2014, Plos Genetics
	Qinghai, China	gwcwq_XinQH11	Wen-Ping Zhang, et al., 2014, Plos Genetics
	Tibet, China	gwcwt_XinTI09	Wen-Ping Zhang, et al., 2014, Plos Genetics
	Liaoning, China	LUPWCHN00003	Guo-Dong Wang et al., 2016, Cell Research
	Inner Mongolia, China	LUPWCHN00001	Guo-Dong Wang et al., 2013, Nature Communications
	Inner Mongolia, China	LUPZCHN00002	Guo-Dong Wang et al., 2016, Cell Research
	Chukotka, Russia	LUPWRUS00002	Guo-Dong Wang et al., 2013, Nature Communications
	Xinjiang, China	LUPWCHN00008	Guo-Dong Wang et al., 2016, Cell Research
	Xinjiang, China	LUPWCHN00009	Guo-Dong Wang et al., 2016, Cell Research
	Xinjiang, China	LUPWCHN00010	Guo-Dong Wang et al., 2016, Cell Research

	Xinjiang, China	LUPWCHN00013	Guo-Dong Wang et al., 2016, Cell Research
	Xinjiang, China	gwcwx_XinXJ24	Wen-Ping Zhang, et al., 2014, Plos Genetics
	Xinjiang, China	gwcwx_XinXJ30	Wen-Ping Zhang, et al., 2014, Plos Genetics
	Altai, Russia	LUPWRUS00001	Guo-Dong Wang et al., 2013, Nature Communications
	Afghan	FAMBAFG00001	Guo-Dong Wang et al., 2016, Cell Research
	Alaskan Malamute	FAMBALM00001	Guo-Dong Wang et al., 2016, Cell Research
	Belgian Malinois	FAMBBEM00001	Guo-Dong Wang et al., 2016, Cell Research
	Chihuahua	FAMBCHI00001	Guo-Dong Wang et al., 2016, Cell Research
	East Siberian Laika	FAMBESL00001	Guo-Dong Wang et al., 2016, Cell Research
	Finnish Lapphund	FAMBFIL00001	Guo-Dong Wang et al., 2016, Cell Research
	Galgo Español	FAMBGAL00001	Guo-Dong Wang et al., 2016, Cell Research
	Gray Norwegian Elkhound	FAMBGNE00001	Guo-Dong Wang et al., 2016, Cell Research
	Greenland dog	FAMBGRD00001	Guo-Dong Wang et al., 2016, Cell Research
	German Shepherd Dog	FAMBGSD00001	Guo-Dong Wang et al., 2016, Cell Research
	Jämthund	FAMBJAM00001	Guo-Dong Wang et al., 2016, Cell Research
	Lapponian Herder	FAMBLAH00001	Guo-Dong Wang et al., 2016, Cell Research
	Mexican hairless	FAMBMEN00001	Guo-Dong Wang et al., 2016, Cell Research
	Peruvian hairless	FAMBPEN00001	Guo-Dong Wang et al., 2016, Cell Research
	Samoyed	FAMBSAM00001	Guo-Dong Wang et al., 2016, Cell Research
	Siberian Husky	FAMBSIH00001	Guo-Dong Wang et al., 2016, Cell Research
	Sloughi	FAMBSLO00001	Guo-Dong Wang et al., 2016, Cell Research
	Swedish Lapphund	FAMBSWL00001	Guo-Dong Wang et al., 2016, Cell Research
Breed dogs	Tibetan Mastiff	FAMBTIM00001	Guo-Dong Wang et al., 2016, Cell Research
	Airedale	ddair_RS74411	D. Marsden Clare et al., 2016 PNAS
	Basenji	ddbas_RS80704	D. Marsden Clare et al., 2016 PNAS
	Border Collie	ddbdr_RS74410	D. Marsden Clare et al., 2016 PNAS
	Border Terrier	ddbdt_RS86407	D. Marsden Clare et al., 2016 PNAS
	Berger Picard	ddber_RS86405	D. Marsden Clare et al., 2016 PNAS
	Black Russian Terrier	ddbrt_RS86399	D. Marsden Clare et al., 2016 PNAS
	Chinese Crested	ddccr_RS88178	D. Marsden Clare et al., 2016 PNAS
	English Spring Spaniel	ddess_RS80702	D. Marsden Clare et al., 2016 PNAS
	Golden Retriever	ddgdr_RS86402	D. Marsden Clare et al., 2016 PNAS
	German Shephard Marsden	ddgsh_RS80703	D. Marsden Clare et al., 2016 PNAS
	Jack Russell Terrier	ddjrt_RS86400	D. Marsden Clare et al., 2016 PNAS
	Jack Russell Terrier	ddjrt_RS86404	D. Marsden Clare et al., 2016 PNAS
	Kerry Blue Terrier	ddkbt_RS74408	D. Marsden Clare et al., 2016 PNAS
	Labrador Retriever	ddlab_RS86398	D. Marsden Clare et al., 2016 PNAS
	Portuguese Podengo	ddppo_RS74409	D. Marsden Clare et al., 2016 PNAS
	Pembroke Welsh Corgi	ddpwc_RS73323	D. Marsden Clare et al., 2016 PNAS
	Pembroke Welsh Corgi	ddpwc_RS86409	D. Marsden Clare et al., 2016 PNAS

	Scottish Terrier	ddsct_RS86393	D. Marsden Clare et al., 2016 PNAS
	Scottish Deerhound	ddsdh_RS86401	D. Marsden Clare et al., 2016 PNAS
	Standard Poodle	ddspo_RS86408	D. Marsden Clare et al., 2016 PNAS
	Shetland Sheepdog	ddssd_RS88649	D. Marsden Clare et al., 2016 PNAS
	Tibetan Terrier	ddtbt_RS86403	D. Marsden Clare et al., 2016 PNAS
	Tibetan Terrier	ddtbt_RS86406	D. Marsden Clare et al., 2016 PNAS
	West Highland White Terrier	ddwhw_RS86397	D. Marsden Clare et al., 2016 PNAS
	Xi'an, Shaanxi, China	FAMICHN00001	Guo-Dong Wang et al., 2013, Nature Communications
	Ya'an, Sichuan, China	FAMICHN00003	Guo-Dong Wang et al., 2013, Nature Communications
	Dalian, Liaoning, China	FAMICHN00004	Guo-Dong Wang et al., 2016, Cell Research
	Gansu, China	FAMICHN00005	Guo-Dong Wang et al., 2016, Cell Research
	Gansu, China	FAMICHN00006	Guo-Dong Wang et al., 2016, Cell Research
	Gansu, China	FAMICHN00007	Guo-Dong Wang et al., 2016, Cell Research
	Hebei, China	FAMICHN00012	Guo-Dong Wang et al., 2016, Cell Research
	Shanxi, China	FAMICHN00014	Guo-Dong Wang et al., 2016, Cell Research
	Shanxi, China	FAMICHN00015	Guo-Dong Wang et al., 2016, Cell Research
	Shaanxi, China	FAMICHN00016	Guo-Dong Wang et al., 2016, Cell Research
	Shaanxi, China	FAMICHN00017	Guo-Dong Wang et al., 2016, Cell Research
	Xinjiang, China	FAMICHN00019	Guo-Dong Wang et al., 2016, Cell Research
Village dogs	Simao, Yunnan, China	FAMICHN00002	Guo-Dong Wang et al., 2013, Nature Communications
	Guangdong, China	FAMICHN00010	Guo-Dong Wang et al., 2016, Cell Research
	Guizhou, China	FAMICHN00011	Guo-Dong Wang et al., 2016, Cell Research
	Yunnan, China	FAMICHN00021	Guo-Dong Wang et al., 2016, Cell Research
	Yunnan, China	FAMICHN00023	Guo-Dong Wang et al., 2016, Cell Research
	Anhui, China	FAMICHN00025	Guo-Dong Wang et al., 2016, Cell Research
	Ibadan, Nigeria	FAMINGR00001	Guo-Dong Wang et al., 2016, Cell Research
	Ondo, Nigeria	FAMINGR00002	Guo-Dong Wang et al., 2016, Cell Research
	Uyo, Nigeria	FAMINGR00003	Guo-Dong Wang et al., 2016, Cell Research
	Taraba State, Nigeria	FAMINGR00004	Guo-Dong Wang et al., 2016, Cell Research
	China/Vietnam border	FAMIVNM00001	Guo-Dong Wang et al., 2016, Cell Research
	China/Vietnam border	FAMIVNM00002	Guo-Dong Wang et al., 2016, Cell Research
	China/Vietnam border	FAMIVNM00003	Guo-Dong Wang et al., 2016, Cell Research
	China/Vietnam border	FAMIVNM00004	Guo-Dong Wang et al., 2016, Cell Research
	China/Vietnam border	FAMIVNM00005	Guo-Dong Wang et al., 2016, Cell Research

Table S3. Z-scores for *D(Fox, Test; X, Y)*. Related to Figure 1 and Figure 2.

D(Andean_fox, W12_Guizhou; P3, P4)

X/Y	Ancient_Taimyr	Iran	Indian	Portugal	Inner_Mongolia	Liaoning	Xinjiang	Altai	Chukotka	Bryansk	Shanxi	China_X	Iberia	Qinghai	Tibet
Ancient_Taimyr		-0.7	0.0	**5.8**	**25.7**	**24.1**	**18.8**	**16.0**	**18.7**	**7.5**	**31.8**	**27.8**	**5.1**	**14.3**	2.4
Iran	0.7		1.0	**7.9**	**28.4**	**25.1**	**22.9**	**17.2**	**21.8**	**9.5**	**34.0**	**28.3**	**7.4**	**15.4**	2.9
Indian	0.0	-1.0		**6.3**	**25.1**	**22.4**	**16.5**	**14.5**	**17.2**	**7.1**	**29.8**	**26.5**	**6.2**	**15.0**	2.5
Portugal	**-5.8**	**-7.9**	**-6.3**		**19.2**	**18.8**	**11.3**	**9.3**	**12.1**	1.1	**28.3**	**23.9**	-0.4	**10.1**	-0.5
Inner_Mongolia	**-25.7**	**-28.4**	**-25.1**	**-19.2**		**3.8**	**-15.0**	**-12.7**	**-8.5**	**-20.5**	**15.1**	**13.8**	**-20.2**	**-3.2**	**-11.8**
Liaoning	**-24.1**	**-25.1**	**-22.4**	**-18.8**	**-3.8**		**-15.0**	**-13.2**	**-10.4**	**-18.0**	**10.9**	**11.3**	**-18.8**	**-5.4**	**-13.4**
Xinjiang	**-18.8**	**-22.9**	**-16.5**	**-11.3**	**15.0**	**15.0**		0.3	**4.4**	**-10.4**	**25.4**	**20.6**	**-10.8**	**5.3**	**-5.3**
Altai	**-16.0**	**-17.2**	**-14.5**	**-9.3**	**12.7**	**13.2**	-0.3		**3.2**	**-8.8**	**22.8**	**19.8**	**-9.6**	**4.8**	**-5.2**
Chukotka	**-18.7**	**-21.8**	**-17.2**	**-12.1**	**8.5**	**10.4**	**-4.4**	**-3.2**		**-11.9**	**20.6**	**18.0**	**-12.8**	2.5	**-6.6**
Bryansk	**-7.5**	**-9.5**	**-7.1**	-1.1	**20.5**	**18.0**	**10.4**	**8.8**	**11.9**		**27.8**	**24.2**	-1.3	**9.5**	-1.0
Shanxi	**-31.8**	**-34.0**	**-29.8**	**-28.3**	**-15.1**	**-10.9**	**-25.4**	**-22.8**	**-20.6**	**-27.8**		1.7	**-29.0**	**-14.3**	**-19.7**
China_X	**-27.8**	**-28.3**	**-26.5**	**-23.9**	**-13.8**	**-11.3**	**-20.6**	**-19.8**	**-18.0**	**-24.2**	-1.7		**-24.3**	**-14.1**	**-20.7**
Iberia	**-5.1**	**-7.4**	**-6.2**	0.4	**20.2**	**18.8**	**10.8**	**9.6**	**12.8**	1.3	**29.0**	**24.3**		**10.2**	-0.3
Qinghai	**-14.3**	**-15.4**	**-15.0**	**-10.1**	**3.2**	**5.4**	**-5.3**	**-4.8**	-2.5	**-9.5**	**14.3**	**14.1**	**-10.2**		**-12.4**
Tibet	-2.4	-2.9	-2.5	0.5	**11.8**	**13.4**	**5.3**	**5.2**	**6.6**	1.0	**19.7**	**20.7**	0.3	**12.4**	

D(Andean_fox, W13_Guizhou; P3, P4)

X/Y	Ancient_Taimyr	Iran	Indian	Portugal	Inner_Mongolia	Liaoning	Xinjiang	Altai	Chukotka	Bryansk	Shanxi	China_X	Iberia	Qinghai	Tibet
Ancient_Taimyr		-0.8	-0.6	**6.5**	**27.1**	**27.3**	**20.3**	**16.0**	**18.8**	**8.8**	**32.2**	**29.8**	**5.0**	**13.2**	**3.4**
Iran	0.8		0.1	**9.1**	**27.8**	**26.8**	**27.5**	**18.4**	**21.9**	**10.5**	**33.5**	**29.0**	**7.0**	**14.4**	**3.9**
Indian	0.6	-0.1		**7.2**	**24.9**	**23.7**	**20.2**	**16.0**	**18.7**	**8.4**	**31.0**	**27.7**	**5.6**	**14.3**	**4.0**
Portugal	**-6.5**	**-9.1**	**-7.2**		**19.1**	**20.3**	**12.3**	**9.5**	**11.9**	1.3	**26.4**	**24.5**	-1.9	**9.3**	0.3
Inner_Mongolia	**-27.1**	**-27.8**	**-24.9**	**-19.1**		**5.5**	**-13.5**	**-11.3**	**-7.1**	**-20.0**	**15.6**	**13.8**	**-21.4**	-2.7	**-10.3**
Liaoning	**-27.3**	**-26.8**	**-23.7**	**-20.3**	**-5.5**		**-15.1**	**-13.6**	**-11.4**	**-20.6**	**9.2**	**9.3**	**-22.1**	**-6.1**	**-12.2**
Xinjiang	**-20.3**	**-27.5**	**-20.2**	**-12.3**	**13.5**	**15.1**		-0.8	**3.8**	**-12.3**	**23.0**	**19.9**	**-15.1**	**4.1**	**-4.7**
Altai	**-16.0**	**-18.4**	**-16.0**	**-9.5**	**11.3**	**13.6**	0.8		**3.6**	**-8.7**	**21.8**	**19.5**	**-10.9**	**4.2**	**-4.3**
Chukotka	**-18.8**	**-21.9**	**-18.7**	**-11.9**	**7.1**	**11.4**	**-3.8**	**-3.6**		**-11.7**	**19.6**	**18.1**	**-14.3**	1.9	**-5.9**
Bryansk	**-8.8**	**-10.5**	**-8.4**	-1.3	**20.0**	**20.6**	**12.3**	**8.7**	**11.7**		**26.6**	**24.8**	**-3.3**	**9.1**	-0.2
Shanxi	**-32.2**	**-33.5**	**-31.0**	**-26.4**	**-15.6**	**-9.2**	**-23.0**	**-21.8**	**-19.6**	**-26.6**		0.5	**-29.7**	**-14.1**	**-18.9**
China_X	**-29.8**	**-29.0**	**-27.7**	**-24.5**	**-13.8**	**-9.3**	**-19.9**	**-19.5**	**-18.1**	**-24.8**	-0.5		**-25.8**	**-13.2**	**-18.3**
Iberia	**-5.0**	**-7.0**	**-5.6**	1.9	**21.4**	**22.1**	**15.1**	**10.9**	**14.3**	**3.3**	**29.7**	**25.8**		**10.6**	1.2
Qinghai	**-13.2**	**-14.4**	**-14.3**	**-9.3**	2.7	**6.1**	**-4.1**	**-4.2**	-1.9	**-9.1**	**14.1**	**13.2**	**-10.6**		**-10.0**

Tibet	-3.4	-3.9	-4.0	-0.3	10.3	12.2	4.7	4.3	5.9	0.2	18.9	18.3	-1.2	10.0	

D(Andean_fox, W2_Jiangxi; P3, P4)

X/Y	Ancient_Taimyr	Iran	Indian	Portugal	Inner_Mongolia	Liaoning	Xinjiang	Altai	Chukotka	Bryansk	Shanxi	China_X	Iberia	Qinghai	Tibet
Ancient_Taimyr		0.3	1.4	3.0	23.3	24.9	18.5	14.9	16.0	5.1	28.5	24.7	3.9	26.0	27.0
Iran	-0.3		1.7	3.3	22.6	24.9	25.5	14.7	17.7	5.4	28.8	23.7	4.5	26.8	27.3
Indian	-1.4	-1.7		1.6	18.7	20.7	16.1	11.7	13.5	2.9	24.3	20.9	2.4	26.5	27.6
Portugal	-3.0	-3.3	-1.6		17.2	19.3	14.6	10.3	12.3	1.5	24.2	20.7	1.1	24.4	25.4
Inner_Mongolia	-23.3	-22.6	-18.7	-17.2		4.2	-9.5	-7.5	-6.6	-19.8	11.1	9.7	-16.0	18.2	21.1
Liaoning	-24.9	-24.9	-20.7	-19.3	-4.2		-13.3	-10.8	-10.7	-20.6	6.0	6.7	-17.9	16.4	19.8
Xinjiang	-18.5	-25.5	-16.1	-14.6	9.5	13.3		-0.2	1.4	-14.9	18.8	15.7	-12.9	21.8	23.5
Altai	-14.9	-14.7	-11.7	-10.3	7.5	10.8	0.2		1.2	-10.4	15.5	14.4	-9.3	21.0	23.1
Chukotka	-16.0	-17.7	-13.5	-12.3	6.6	10.7	-1.4	-1.2		-12.2	16.5	14.3	-10.7	20.1	22.2
Bryansk	-5.1	-5.4	-2.9	-1.5	19.8	20.6	14.9	10.4	12.2		26.0	22.2	-0.3	24.7	25.7
Shanxi	-28.5	-28.8	-24.3	-24.2	-11.1	-6.0	-18.8	-15.5	-16.5	-26.0		1.7	-23.1	13.1	17.1
China_X	-24.7	-23.7	-20.9	-20.7	-9.7	-6.7	-15.7	-14.4	-14.3	-22.2	-1.7		-19.4	11.9	16.1
Iberia	-3.9	-4.5	-2.4	-1.1	16.0	17.9	12.9	9.3	10.7	0.3	23.1	19.4		23.9	25.2
Qinghai	-26.0	-26.8	-26.5	-24.4	-18.2	-16.4	-21.8	-21.0	-20.1	-24.7	-13.1	-11.9	-23.9		12.4
Tibet	-27.0	-27.3	-27.6	-25.4	-21.1	-19.8	-23.5	-23.1	-22.2	-25.7	-17.1	-16.1	-25.2	-12.4	

D(Andean_fox, W6_Jilin; P3, P4)

X/Y	Ancient_Taimyr	Iran	Indian	Portugal	Inner_Mongolia	Liaoning	Xinjiang	Altai	Chukotka	Bryansk	Shanxi	China_X	Iberia	Qinghai	Tibet
Ancient_Taimyr		-1.7	-2.0	5.4	25.7	22.3	15.9	15.1	18.2	7.6	24.1	21.5	6.1	6.8	-1.2
Iran	1.7		-0.8	9.3	28.8	24.3	25.5	15.9	22.5	10.6	26.2	21.8	10.4	8.4	-0.3
Indian	2.0	0.8		7.6	24.0	22.0	18.3	14.0	19.4	8.8	22.6	20.7	8.9	8.6	-0.1
Portugal	-5.4	-9.3	-7.6		18.6	17.2	10.5	8.3	14.1	1.8	18.2	15.5	0.3	3.4	-4.1
Inner_Mongolia	-25.7	-28.8	-24.0	-18.6		3.9	-15.8	-10.0	-5.3	-19.0	3.0	2.4	-20.2	-8.9	-14.4
Liaoning	-22.3	-24.3	-22.0	-17.2	-3.9		-14.3	-11.2	-7.2	-16.9	-1.2	-1.1	-18.3	-10.9	-16.0
Xinjiang	-15.9	-25.5	-18.3	-10.5	15.8	14.3		1.9	7.2	-7.9	15.3	12.1	-11.6	-1.7	-8.7
Altai	-15.1	-15.9	-14.0	-8.3	10.0	11.2	-1.9		3.7	-8.1	11.8	9.2	-9.2	-2.5	-8.8
Chukotka	-18.2	-22.5	-19.4	-14.1	5.3	7.2	-7.2	-3.7		-12.0	6.9	5.9	-13.6	-5.2	-11.2
Bryansk	-7.6	-10.6	-8.8	-1.8	19.0	16.9	7.9	8.1	12.0		19.1	15.9	-1.7	2.1	-4.9
Shanxi	-24.1	-26.2	-22.6	-18.2	-3.0	1.2	-15.3	-11.8	-6.9	-19.1		0.0	-20.0	-10.6	-15.3
China_X	-21.5	-21.8	-20.7	-15.5	-2.4	1.1	-12.1	-9.2	-5.9	-15.9	0.0		-17.3	-10.3	-15.1
Iberia	-6.1	-10.4	-8.9	-0.3	20.2	18.3	11.6	9.2	13.6	1.7	20.0	17.3		3.2	-4.2
Qinghai	-6.8	-8.4	-8.6	-3.4	8.9	10.9	1.7	2.5	5.2	-2.1	10.6	10.3	-3.2		-10.1
Tibet	1.2	0.3	0.1	4.1	14.4	16.0	8.7	8.8	11.2	4.9	15.3	15.1	4.2	10.1	

D(Andean_fox, W7_Zhejiang; P3, P4)

X/Y	Ancient_Taimyr	Iran	Indian	Portugal	Inner_Mongolia	Liaoning	Xinjiang	Altai	Chukotka	Bryansk	Shanxi	China_X	Iberia	Qinghai	Tibet
Ancient_Taimyr		-1.0	-0.6	5.3	21.7	23.4	14.4	11.7	14.6	4.6	32.6	29.1	5.2	16.6	7.3
Iran	1.0		0.2	8.9	26.0	27.1	22.1	14.9	20.1	7.9	38.0	30.4	8.9	19.7	8.6
Indian	0.6	-0.2		7.1	21.5	22.9	16.0	12.6	15.8	5.8	31.7	28.2	7.0	18.9	8.5
Portugal	-5.3	-8.9	-7.1		15.3	17.6	8.1	6.3	9.8	-0.9	28.6	24.0	-0.4	13.2	4.4
Inner_Mongolia	-21.7	-26.0	-21.5	-15.3		4.7	-13.2	-11.8	-6.9	-19.0	16.6	14.9	-16.9	1.8	-4.4
Liaoning	-23.4	-27.1	-22.9	-17.6	-4.7		-16.5	-14.4	-10.6	-20.3	11.1	12.5	-19.6	-1.6	-6.8
Xinjiang	-14.4	-22.1	-16.0	-8.1	13.2	16.5		-0.5	4.3	-10.5	28.6	23.2	-9.0	9.7	1.1
Altai	-11.7	-14.9	-12.6	-6.3	11.8	14.4	0.5		3.7	-8.3	25.9	22.1	-6.8	9.0	1.2
Chukotka	-14.6	-20.1	-15.8	-9.8	6.9	10.6	-4.3	-3.7		-11.5	21.1	19.1	-10.2	6.1	-0.7
Bryansk	-4.6	-7.9	-5.8	0.9	19.0	20.3	10.5	8.3	11.5		31.2	26.5	0.6	13.8	4.8
Shanxi	-32.6	-38.0	-31.7	-28.6	-16.6	-11.1	-28.6	-25.9	-21.1	-31.2		2.6	-29.4	-9.8	-12.8
China_X	-29.1	-30.4	-28.2	-24.0	-14.9	-12.5	-23.2	-22.1	-19.1	-26.5	-2.6		-25.1	-10.7	-14.8
Iberia	-5.2	-8.9	-7.0	0.4	16.9	19.6	9.0	6.8	10.2	-0.6	29.4	25.1		13.3	4.6
Qinghai	-16.6	-19.7	-18.9	-13.2	-1.8	1.6	-9.7	-9.0	-6.1	-13.8	9.8	10.7	-13.3		-8.3
Tibet	-7.3	-8.6	-8.5	-4.4	4.4	6.8	-1.1	-1.2	0.7	-4.8	12.8	14.8	-4.6	8.3	

D(Andean_fox, W9_Heilongjiang; P3, P4)

X/Y	Ancient_Taimyr	Iran	Indian	Portugal	Inner_Mongolia	Liaoning	Xinjiang	Altai	Chukotka	Bryansk	Shanxi	China_X	Iberia	Qinghai	Tibet
Ancient_Taimyr		-1.4	-1.1	5.5	23.1	24.5	15.3	13.1	16.0	7.7	23.4	21.0	5.4	5.8	-2.4
Iran	1.4		0.0	9.1	25.4	25.6	25.7	14.7	20.5	9.3	24.4	21.8	9.3	7.8	-1.7
Indian	1.1	0.0		6.6	21.5	22.8	16.7	12.5	16.2	7.2	21.3	19.7	7.1	7.3	-1.7
Portugal	-5.5	-9.1	-6.6		15.9	19.4	9.7	7.5	12.2	1.6	16.1	14.7	-0.3	2.6	-5.1
Inner_Mongolia	-23.1	-25.4	-21.5	-15.9		7.1	-12.5	-9.4	-5.3	-16.6	2.3	3.0	-18.5	-9.8	-15.1
Liaoning	-24.5	-25.6	-22.8	-19.4	-7.1		-16.0	-14.0	-10.4	-19.8	-5.1	-3.8	-21.1	-13.2	-17.3
Xinjiang	-15.3	-25.7	-16.7	-9.7	12.5	16.0		0.8	6.1	-7.1	12.9	11.7	-11.3	-3.0	-9.8
Altai	-13.1	-14.7	-12.5	-7.5	9.4	14.0	-0.8		4.0	-7.5	11.4	10.2	-8.6	-2.9	-9.3
Chukotka	-16.0	-20.5	-16.2	-12.2	5.3	10.4	-6.1	-4.0		-10.2	7.0	6.9	-12.8	-5.8	-11.6
Bryansk	-7.7	-9.3	-7.2	-1.6	16.6	19.8	7.1	7.5	10.2		17.2	15.8	-1.8	1.3	-5.8
Shanxi	-23.4	-24.4	-21.3	-16.1	-2.3	5.1	-12.9	-11.4	-7.0	-17.2		1.0	-18.5	-10.8	-15.7
China_X	-21.0	-21.8	-19.7	-14.7	-3.0	3.8	-11.7	-10.2	-6.9	-15.8	-1.0		-17.1	-10.7	-15.6
Iberia	-5.4	-9.3	-7.1	0.3	18.5	21.1	11.3	8.6	12.8	1.8	18.5	17.1		2.6	-5.0
Qinghai	-5.8	-7.8	-7.3	-2.6	9.8	13.2	3.0	2.9	5.8	-1.3	10.8	10.7	-2.6		-10.5
Tibet	2.4	1.7	1.7	5.1	15.1	17.3	9.8	9.3	11.6	5.8	15.7	15.6	5.0	10.5	

Table S4. F3 tests among the SC, NA, and Tibetan gray wolves. Related to Figure 1 and Figure 2.

Source 1	Source 1	Target	f_3	std. err	Z	SNPs
Tibetan	SC	Jiangxi	-0.08023	0.007068	-11.352	2638661
Tibetan	NA	Jiangxi	-0.06734	0.007366	-9.141	2478583
Tibetan	SC	Qinghai	-0.09735	0.005096	-19.101	2631539
Tibetan	NA	Qinghai	-0.09298	0.00522	-17.811	2488007

Table S5. Z-scores for *D(Fox, X; Test, Y)*. Related to Figure 1 and Figure 2.

D(Andean_fox, P2; W12_Guizhou, P4)

X/Y	Ancient_Taimyr	Iran	Indian	Portugal	Inner_Mongolia	Liaoning	Xinjiang	Altai	Chukotka	Bryansk	Shanxi	China_X	Iberia	Qinghai	Tibet
Ancient_Taimyr		-5.7	-6.7	3.8	2.7	2.0	0.2	2.4	4.1	2.6	2.1	1.8	2.8	-8.5	-12.8
Iran	-4.1		38.2	14.5	4.4	2.5	14.5	11.5	8.0	14.9	1.5	1.5	14.8	-6.1	-10.8
Indian	-5.2	36.2		9.1	3.6	1.5	11.4	8.9	6.2	8.9	0.4	-0.2	8.6	-4.5	-8.7
Portugal	-1.8	8.2	4.4		4.6	2.9	11.9	8.3	8.3	19.8	1.0	-0.6	30.5	-7.4	-15.0
Inner_Mongolia	-22.4	-25.8	-21.6	-14.2		2.2	-9.6	-7.0	-3.4	-13.2	2.2	2.9	-17.6	-10.4	-14.7
Liaoning	-21.8	-24.4	-20.8	-16.7	-1.7		-12.7	-10.5	-7.0	-15.0	1.3	1.8	-16.5	-10.9	-15.3
Xinjiang	-18.2	-6.7	-6.0	1.2	7.5	3.7		8.1	4.8	1.3	3.0	2.7	-2.0	-8.0	-12.1
Altai	-11.7	-5.0	-4.6	0.7	5.0	2.1	6.3		5.0	3.1	2.3	3.4	0.4	-6.7	-11.7
Chukotka	-12.3	-11.3	-10.1	-2.2	5.2	4.6	0.1	1.8		-2.5	1.7	2.8	-4.5	-8.5	-13.2
Bryansk	-4.3	7.5	3.4	20.3	4.8	3.4	10.2	10.5	7.6		1.9	1.8	18.5	-7.8	-12.8
Shanxi	-29.9	-32.0	-29.5	-26.9	-13.4	-9.5	-22.9	-20.6	-19.7	-25.0		4.2	-28.4	-14.0	-18.7
China_X	-27.1	-28.8	-28.0	-24.8	-12.3	-9.7	-20.6	-18.0	-16.9	-23.1	2.3		-24.3	-13.8	-19.9
Iberia	-2.5	7.1	3.1	30.3	2.8	3.2	8.4	9.1	7.1	19.7	1.9	1.2		-7.9	-13.2
Qinghai	-23.7	-22.7	-18.7	-18.6	-6.1	-4.7	-14.4	-11.4	-11.9	-18.8	0.3	-0.8	-21.3		24.1
Tibet	-19.4	-18.7	-14.6	-17.9	-2.4	-1.8	-8.4	-8.0	-8.3	-17.1	2.0	0.7	-17.8	34.6	

D(Andean_fox, P2; W13_Guizhou, P4)

X/Y	Ancient_Taimyr	Iran	Indian	Portugal	Inner_Mongolia	Liaoning	Xinjiang	Altai	Chukotka	Bryansk	Shanxi	China_X	Iberia	Qinghai	Tibet
Ancient_Taimyr		-5.3	-5.7	3.7	2.7	2.1	0.3	2.3	3.5	2.5	1.9	1.8	2.5	-7.8	-12.4
Iran	-4.4		35.9	14.8	4.2	2.4	14.7	11.3	7.7	14.3	1.4	1.2	13.1	-6.4	-11.3
Indian	-4.9	34.8		9.8	4.1	2.0	12.5	9.2	6.7	9.0	1.0	0.4	8.0	-4.1	-8.8
Portugal	-1.8	8.2	4.2		4.3	2.8	11.4	8.0	8.1	20.2	0.8	-0.7	29.6	-7.9	-15.6
Inner_Mongolia	-21.9	-24.4	-18.8	-12.7		3.5	-7.7	-6.0	-2.2	-12.6	3.6	4.2	-15.1	-9.6	-14.3
Liaoning	-22.3	-24.7	-20.9	-17.5	-2.4		-12.8	-11.4	-8.0	-15.9	0.5	1.3	-17.4	-10.8	-15.1
Xinjiang	-16.8	-7.3	-6.3	0.3	5.6	2.5		6.9	3.7	0.4	1.6	1.6	-2.5	-8.8	-12.8
Altai	-10.7	-5.1	-4.2	0.8	5.0	2.2	6.4		5.1	3.2	2.4	3.4	0.4	-6.6	-11.6
Chukotka	-11.7	-11.6	-9.7	-2.5	4.6	4.0	-0.3	1.5		-2.8	1.3	2.5	-4.4	-8.8	-14.1
Bryansk	-4.2	7.1	2.9	21.2	4.9	3.2	9.9	10.6	7.3		1.7	1.4	18.2	-8.9	-14.2
Shanxi	-28.3	-30.6	-28.3	-24.9	-11.9	-8.6	-21.0	-19.3	-19.4	-23.9		4.2	-24.9	-13.4	-18.5
China_X	-27.5	-27.9	-26.5	-24.7	-10.8	-8.0	-19.7	-16.4	-16.1	-22.4	3.7		-23.3	-13.0	-18.4
Iberia	-1.7	7.9	3.6	31.0	3.8	4.2	9.7	9.8	7.4	20.1	2.8	2.0		-7.3	-13.7
Qinghai	-22.2	-21.0	-16.5	-17.1	-5.3	-4.2	-12.9	-10.5	-10.7	-18.1	0.7	-0.3	-18.1		23.7
Tibet	-19.9	-18.7	-14.6	-18.5	-3.9	-3.0	-8.8	-8.8	-9.2	-17.5	0.5	-0.7	-18.3	33.5	

D(Andean_fox, P2; W2_Jiangxi, P4)

X/Y	Ancient_Taimyr	Iran	Indian	Portugal	Inner_Mongolia	Liaoning	Xinjiang	Altai	Chukotka	Bryansk	Shanxi	China_X	Iberia	Qinghai	Tibet
Ancient_Taimyr		3.4	2.2	8.5	8.7	8.7	7.5	8.2	8.3	8.0	8.4	8.4	8.2	-0.5	-8.7
Iran	3.2		33.5	16.2	9.3	8.3	15.3	13.3	10.9	16.2	7.3	7.3	14.6	0.9	-6.8
Indian	1.2	31.5		12.5	8.2	7.0	14.1	11.9	10.0	11.6	6.2	5.5	10.8	1.6	-4.8
Portugal	6.1	14.1	11.2		11.1	10.3	17.1	13.5	14.8	23.4	8.8	8.0	33.6	0.9	-9.0
Inner_Mongolia	-6.2	-6.0	-5.1	-0.8		10.3	5.0	4.6	7.3	-0.3	10.5	11.2	-2.3	1.8	-8.2
Liaoning	-9.0	-9.6	-9.3	-4.5	7.4		0.5	0.3	3.8	-3.7	9.3	9.9	-4.3	-0.6	-9.6
Xinjiang	-3.2	3.9	3.8	8.2	11.7	10.0		12.2	10.5	8.1	9.7	10.0	6.1	1.3	-7.1
Altai	-1.3	3.2	3.3	6.6	9.8	8.0	11.2		9.7	8.2	8.6	9.4	6.3	1.0	-7.0
Chukotka	-1.2	0.2	0.3	5.9	12.0	12.0	9.0	9.1		5.7	9.8	10.2	4.3	1.1	-7.6
Bryansk	5.0	13.1	9.8	23.3	11.4	11.0	15.4	15.5	13.2		10.1	9.8	20.8	0.9	-8.0
Shanxi	-12.1	-12.9	-12.8	-8.9	3.0	4.9	-4.2	-3.5	-2.1	-8.1		14.5	-8.5	-0.5	-10.8
China_X	-12.0	-13.2	-13.2	-10.4	2.0	4.0	-5.0	-3.6	-2.4	-8.6	13.3		-8.9	-2.3	-12.0
Iberia	5.1	10.9	8.4	31.4	8.7	9.3	12.6	12.7	11.0	20.2	8.6	7.8		0.1	-9.4
Qinghai	-28.3	-28.3	-26.2	-25.1	-18.3	-18.0	-23.2	-21.8	-21.8	-25.5	-15.4	-15.4	-26.1		16.9
Tibet	-34.5	-33.2	-31.8	-33.7	-27.0	-26.9	-29.5	-29.3	-29.4	-32.4	-25.6	-26.7	-33.4	3.4	

D(Andean_fox, P2; W7_Zhejiang, P4)

X/Y	Ancient_Taimyr	Iran	Indian	Portugal	Inner_Mongolia	Liaoning	Xinjiang	Altai	Chukotka	Bryansk	Shanxi	China_X	Iberia	Qinghai	Tibet
Ancient_Taimyr		48.6	41.7	49.2	56.0	51.6	61.0	50.7	52.2	47.2	54.3	48.3	46.8	31.9	18.1
Iran	42.9		81.3	62.1	59.3	55.9	80.2	60.5	62.2	59.0	57.5	52.3	65.3	35.4	21.8
Indian	36.5	80.5		51.9	49.4	48.9	74.4	52.0	57.1	48.1	50.0	45.0	54.6	34.1	22.5
Portugal	38.5	57.4	45.5		48.3	48.4	73.2	49.5	57.1	54.9	48.8	43.4	58.9	28.7	17.2
Inner_Mongolia	28.8	37.5	32.1	39.2		57.4	62.1	47.8	52.4	38.1	60.4	56.9	37.1	36.3	18.3
Liaoning	23.3	27.3	22.7	30.3	44.5		43.3	34.7	42.5	28.9	49.7	46.2	29.7	30.2	14.9
Xinjiang	40.2	60.5	54.5	60.5	74.7	68.9		68.3	68.6	55.6	71.3	63.2	59.6	39.5	21.7
Altai	35.9	49.8	44.7	47.8	62.8	53.7	71.2		58.5	49.0	60.9	53.3	48.0	33.6	19.2
Chukotka	32.1	41.7	36.5	43.9	57.0	58.6	60.0	47.5		41.8	57.0	52.9	42.9	32.4	16.2
Bryansk	43.1	64.4	50.8	60.5	61.7	59.1	73.4	61.0	59.9		62.8	52.9	62.4	31.3	17.7
Shanxi	12.9	14.6	12.5	19.3	36.8	35.5	30.9	26.5	30.6	19.7		38.1	20.2	23.0	11.0
China_X	9.0	9.4	8.4	12.3	27.2	30.3	21.9	19.5	21.9	13.6	32.8		12.7	16.6	8.0
Iberia	41.3	63.0	52.6	60.9	54.8	55.0	71.6	57.6	55.6	61.8	57.7	46.8		31.1	16.9
Qinghai	15.1	19.5	17.0	18.6	35.2	35.0	38.4	27.0	32.3	21.3	41.7	34.8	21.3		44.3
Tibet	14.4	20.1	19.2	17.0	33.8	33.7	35.6	26.1	26.2	20.7	36.1	33.9	17.9	54.2	

D(Andean_fox, P2; W6_Jilin, P4)

X/Y	Ancient_Taimyr	Iran	Indian	Portugal	Inner_Mongolia	Liaoning	Xinjiang	Altai	Chukotka	Bryansk	Shanxi	China_X	Iberia	Qinghai	Tibet
Ancient_Taimyr		-6.1	-7.7	3.0	1.6	0.8	-1.0	1.5	2.8	2.0	1.0	0.9	2.2	-8.6	-13.3
Iran	-4.1		35.5	12.8	5.2	2.6	13.4	13.1	6.7	18.9	1.5	0.9	14.3	-5.3	-10.0
Indian	-4.8	31.9		8.1	6.1	3.0	11.2	12.0	6.2	12.8	1.6	0.5	9.0	-3.0	-7.8
Portugal	-2.6	6.1	2.8		4.8	2.5	9.1	8.8	7.3	23.1	0.2	-2.0	30.0	-6.7	-14.6
Inner_Mongolia	-25.2	-24.1	-19.8	-13.3		2.9	-8.8	-7.8	-3.2	-14.4	3.1	3.6	-17.0	-9.0	-13.8
Liaoning	-22.6	-24.2	-21.0	-15.6	-1.2		-12.4	-11.7	-6.3	-16.2	1.8	2.3	-16.5	-9.4	-14.9
Xinjiang	-18.7	-7.2	-6.5	1.2	7.1	3.6		8.3	4.5	1.5	2.7	2.2	-1.9	-8.0	-12.1
Altai	-13.1	-5.9	-5.3	-0.5	3.0	0.3	4.0		3.2	1.9	0.4	1.5	-0.9	-7.5	-12.6
Chukotka	-14.6	-13.3	-12.4	-4.1	2.4	1.5	-3.0	-0.7		-5.1	-1.3	-0.2	-6.5	-10.6	-15.3
Bryansk	-5.9	5.6	1.6	18.6	3.8	1.6	8.6	10.4	6.4		0.1	-0.4	17.5	-8.7	-14.0
Shanxi	-24.8	-26.0	-23.1	-18.1	0.0	3.3	-12.6	-12.0	-8.7	-19.1		16.1	-19.8	-4.0	-11.0
China_X	-22.2	-24.0	-22.3	-17.9	0.6	3.5	-12.4	-9.1	-6.6	-16.4	16.3		-17.8	-5.0	-11.7
Iberia	-4.2	6.0	1.7	31.3	1.5	2.0	7.8	9.2	5.9	20.4	0.3	-0.6		-9.1	-14.6
Qinghai	-21.0	-14.3	-10.6	-10.4	1.6	2.4	-6.2	-6.7	-4.8	-16.5	8.5	6.4	-14.1		27.1
Tibet	-18.3	-16.6	-11.3	-14.9	2.5	2.3	-4.0	-5.1	-5.2	-15.9	6.8	4.3	-15.9	36.9	

D(Andean_fox, P2; W9_Heilongjiang, P4)

X/Y	Ancient_Taimyr	Iran	Indian	Portugal	Inner_Mongolia	Liaoning	Xinjiang	Altai	Chukotka	Bryansk	Shanxi	China_X	Iberia	Qinghai	Tibet
Ancient_Taimyr		-5.1	-7.2	2.7	2.3	1.5	0.1	2.0	3.5	2.5	1.7	1.4	2.6	-7.9	-12.5
Iran	-3.7		35.6	12.9	5.0	2.8	14.0	12.5	7.0	19.5	1.4	0.6	15.2	-5.0	-9.8
Indian	-5.5	29.8		7.1	5.1	2.1	10.5	9.9	5.4	10.9	0.7	-0.3	8.2	-3.2	-7.8
Portugal	-2.9	6.2	2.8		4.7	2.4	9.5	8.6	7.4	24.5	-0.5	-2.5	29.9	-7.0	-14.8
Inner_Mongolia	-23.3	-21.5	-18.5	-11.4		4.0	-6.7	-6.6	-1.9	-13.0	4.2	4.7	-15.7	-8.1	-12.9
Liaoning	-23.2	-24.0	-22.2	-17.4	-3.6		-13.7	-13.6	-8.3	-17.8	-0.8	-0.3	-17.7	-11.3	-15.5
Xinjiang	-17.7	-6.5	-6.1	1.1	6.7	3.8		8.3	4.8	1.3	2.7	1.8	-1.6	-7.9	-11.7
Altai	-12.3	-5.1	-5.2	-0.2	4.0	1.0	5.4		4.0	2.2	1.2	2.1	-0.3	-6.6	-11.5
Chukotka	-12.8	-12.3	-11.2	-3.2	3.7	3.0	-1.5	0.3		-4.2	-0.2	1.1	-5.1	-9.5	-14.5
Bryansk	-5.8	5.5	1.6	18.5	3.9	1.9	8.5	9.8	6.2		-0.5	-0.8	17.5	-9.2	-14.2
Shanxi	-24.3	-24.2	-22.8	-17.6	1.5	4.9	-11.3	-9.8	-7.6	-18.8		17.0	-18.9	-3.1	-10.1
China_X	-21.9	-24.1	-22.2	-18.4	1.4	4.1	-12.1	-9.4	-6.2	-18.5	16.2		-18.5	-4.6	-11.2
Iberia	-3.2	7.3	2.4	31.1	2.2	2.9	9.1	8.8	6.2	21.5	0.7	-0.4		-8.9	-14.1
Qinghai	-19.2	-12.7	-9.5	-9.6	3.5	3.8	-4.8	-5.4	-3.9	-16.7	9.7	7.3	-12.9		27.7
Tibet	-15.8	-13.4	-9.5	-13.1	4.6	4.4	-1.1	-3.0	-3.1	-13.5	8.2	6.5	-14.5	37.2	

Table S6. D values and Z-scores for *D(Fox, Dhole/Jackal; Test, Jackal/Coyote/Red_wolf/Zhejiang)*. Related to Figure 1 and Figure 2.

D(Fox, Jackal; P3, P4)								
	D-value				Z-score			
P3/P4	Dhole	Coyote	Red_Wolf	W7_Zhejiang	Dhole	Coyote	Red_Wolf	W7_Zhejiang
Dhole		0.624	0.619	0.527		100.0	100.0	100.0
Coyote	-0.624		0.017	-0.134	-100.0		6.4	-34.1
Red_Wolf	-0.619	-0.017		-0.147	-100.0	-6.4		-37.0
Ancient_Taimyr	-0.619	-0.042	-0.030	-0.189	-100.0	-16.2	-10.7	-39.7
W12_Guizhou	-0.614	-0.035	-0.022	-0.247	-100.0	-14.3	-8.9	-49.5
W13_Guizhou	-0.612	-0.033	-0.021	-0.205	-100.0	-13.4	-8.7	-41.8
W2_Jiangxi	-0.611	-0.033	-0.021	-0.194	-100.0	-12.9	-7.8	-42.7
W7_Zhejiang	-0.527	0.134	0.147		-100.0	34.1	37.0	
W6_Jilin	-0.612	-0.030	-0.019	-0.179	-100.0	-11.0	-6.4	-33.6
W9_Heilongjiang	-0.606	-0.030	-0.017	-0.170	-100.0	-10.5	-5.6	-29.9
Indian	-0.612	-0.037	-0.025	-0.179	-100.0	-12.8	-9.4	-43.5
Iran	-0.609	-0.035	-0.023	-0.175	-100.0	-14.3	-10.2	-50.6
Portugal	-0.611	-0.038	-0.026	-0.186	-100.0	-13.3	-9.9	-41.7
Inner_Mongolia	-0.610	-0.035	-0.023	-0.188	-100.0	-15.1	-9.5	-45.9
Liaoning	-0.612	-0.038	-0.026	-0.192	-100.0	-16.1	-10.7	-46.1
Xinjiang	-0.610	-0.036	-0.024	-0.186	-100.0	-16.5	-11.5	-55.5
Altai	-0.612	-0.038	-0.026	-0.184	-100.0	-15.3	-9.9	-44.3
Chukotka	-0.611	-0.036	-0.024	-0.186	-100.0	-14.5	-9.5	-45.5
Bryansk	-0.612	-0.039	-0.027	-0.181	-100.0	-15.4	-10.3	-42.0
Shanxi	-0.611	-0.037	-0.025	-0.191	-100.0	-16.4	-10.4	-45.0
China_X	-0.610	-0.038	-0.026	-0.195	-100.0	-15.0	-9.5	-40.5
Qinghai	-0.612	-0.037	-0.025	-0.193	-100.0	-13.3	-9.3	-43.1
Tibet	-0.610	-0.032	-0.019	-0.183	-100.0	-12.0	-6.9	-39.6

D(Fox, Dhole; P3, P4)								
	D-Value				Z-score			
P3/P4	Jackal	Coyote	Red_Wolf	W7_Zhejiang	Jackal	Coyote	Red_Wolf	W7_Zhejiang
Jackal		-0.004	-0.012	-0.117		-1.5	-3.9	-20.2
Coyote	0.004		-0.009	-0.114	1.5		-3.2	-19.2
Red_Wolf	0.012	0.009		-0.109	3.9	3.2		-17.8
Ancient_Taimyr	0.014	0.013	0.007	-0.109	4.6	4.1	2.1	-14.2
W12_Guizhou	0.020	0.017	0.011	-0.150	6.5	5.7	3.7	-19.4
W13_Guizhou	0.019	0.017	0.010	-0.125	5.9	5.4	3.2	-18.1

W2_Jiangxi	0.020	0.017	0.010	-0.119	6.6	5.6	3.4	-17.8
W7_Zhejiang	0.117	0.114	0.109		20.2	19.2	17.8	
W6_Jilin	0.028	0.024	0.017	-0.102	7.5	7.2	4.7	-11.7
W9_Heilongjiang	0.026	0.024	0.017	-0.108	7.0	6.3	4.2	-12.1
Indian	0.016	0.013	0.006	-0.113	5.6	4.7	2.2	-17.3
Iran	0.016	0.013	0.006	-0.108	6.3	5.4	2.6	-19.7
Portugal	0.015	0.012	0.005	-0.117	4.9	4.3	1.8	-18.0
Inner_Mongolia	0.015	0.012	0.005	-0.114	5.6	4.6	2.1	-19.0
Liaoning	0.015	0.013	0.005	-0.114	5.2	4.4	1.9	-19.0
Xinjiang	0.014	0.011	0.004	-0.116	5.4	4.6	1.6	-22.4
Altai	0.013	0.010	0.003	-0.113	4.4	3.5	1.0	-18.2
Chukotka	0.017	0.014	0.007	-0.117	5.6	4.9	2.5	-19.8
Bryansk	0.015	0.012	0.005	-0.114	5.0	3.9	1.6	-17.9
Shanxi	0.013	0.010	0.003	-0.124	4.4	3.6	1.0	-20.5
China_X	0.017	0.014	0.007	-0.115	5.5	4.8	2.3	-17.3
Qinghai	0.015	0.012	0.005	-0.117	5.2	4.5	1.9	-18.1
Tibet	0.017	0.015	0.007	-0.112	5.5	4.7	2.5	-17.0

Transparent Methods

Detailed methods of this paper include the following:

- CONTACT FOR RESOURCE SHARING
- EXPERIMENTAL MODEL AND SUBJECT DETAILS
- METHOD DETAILS
- + Extraction
- + Library preparation
- + Sequencing and data processing
- + Genotype calling
- QUANTIFICATION AND STATISTICAL ANALYSIS
- + Phylogeny, maximum likelihood and neighbor joining
- + f3-statistics
- + D-statistics
- + TreeMix
- + F4-ratio test
- + Admixture Graph

- DATA AND SOFTWARE AVAILABILITY

- CONTACT FOR RESOURCE SHARING

Further information and requests for resources and reagents should be directed to and will be fulfilled by the Lead Contact Ya-Ping Zhang (zhangyp@mail.kiz.ac.cn).

- METHOD DETAILS

- + **Extraction**

Six historical wolf skin samples were collected from two museums: National Zoological Museum of China in Beijing, and Kunming Natural History Museum of Zoology in Yunnan. The Zhejiang wolf (W7_Zhejiang) was collected from Lin'an, Zhejiang province in 1974 and the Jiangxi wolf (W2_Jiangxi) was collected from Jiangxi province in May 1974. Both regions are located in the downstream region of the Yangtze River in South China. The two Guizhou wolves (W12_Guizhou and W13_Guizhou) were collected from Guizhou province in South China near Southeast Asia in 1963. The final two wolves sampled in this study (W9_Heilongjiang and W6_Jilin) were collected from Northeast China (Baoqing, Heilongjiang province on Jan 24th, 1957, and Baicheng, Jilin province on Feb 11th, 1957, respectively) (Figure 1A). All samples were treated by As2O3 for storage.

We extracted DNA from these six different skin samples. Each sample was shaved with a sterilized razor blade to remove the fur. For each skin sample, we cut 25 mg into small pieces of size <1 cubic millimeter, using sterilized scissors between each sample, placing the pieces into a PCR clean 2.0 mL DNA LoBind tube (Eppendorf, cat. No. 30108078). For each sample, we rinsed the pieces in 70% ethanol (Sigma Aldrich, cat. No. E7023). The mixture was vortexed at maximum speed for one minute and then spun at 13,200 rpm in a table centrifuge for one minute. Finally, we removed the resulting supernatant. We repeated these steps three times and let the tube stand for five minutes at 40°C for complete ethanol evaporation. We used the remaining skin sample in each tube to prepare 50 uL of DNA extract per sample, using the DNA extraction method described in Dabney et al (Dabney et al., 2013). Preparation of samples was performed in a clean room at the Laboratory on Molecular Paleontology, at the Institute of Vertebrate Paleontology and Paleoanthropology

(IVPP), Chinese Academy of Sciences, Beijing, China. All used tubes and other experiment materials were UV irradiated for 40 mins, and the used reagents were UV irradiated for 20 mins. All laboratory procedures were conducted using contamination controls, such as use of full body coverings, bleach decontamination, and UV irradiation of tools and work area before and between uses.

- + **Library preparation**

Thirty-five libraries were produced using a double stranded library preparation protocol (Kircher et al., 2012; Meyer and Kircher, 2010) (Table S1). Libraries were all treated with uracil-DNA-glycosylase (UDG) and endonuclease (Endo VIII) to remove characteristic ancient DNA deamination (Briggs et al., 2007). All 35 libraries were PCR amplified using AccuPrimePfx DNA polymerase (Life Technologies) (Dabney and Meyer, 2012). Sample-specific indexes were introduced into both the P5 and P7 adaptors during this library amplification to make it possible to distinguish samples from the new libraries from any other library (Kircher et al., 2012). Library concentrations were determined using a NanoDrop 2000 spectrophotometer and a DNA-1000 chip on the Agilent Bioanalyzer 2100.

- + **Sequencing and data processing**

We sequenced the libraries using 2×150 bp reads on an Illumina HiSeq Xten platform. Reads were demultiplexed according to the expected index pairs (Table S1) allowing one mismatch on each pair of reads. The resulting paired reads were then merged into a single read, requiring an overlap of at least 11 bp (with one mismatch allowed), using a modified form of SeqPrep (John, 2011), in which higher quality bases (and scores) are used in the overlap region. After stripping adapters, merged reads were aligned as unpaired molecules using BWA (v 0.6.1) using samse (Li and Durbin, 2009). Reads were considered duplicates if they had the same start and end positions, and all duplicates were removed with bam-rmdup (https://github.com/mpieva/biohazard-tools), keeping only the read for each set of duplicates with the highest quality bases (Table S1).

- + **Genotype calling**

We merged the SNPs from Wang et al (Wang et al., 2016) and Marsden et al (Marsden et al., 2016), excluding any variants where the alleles did not match and any SNPs only present in one of the datasets. Together, this merging yielded 13.74 million SNPs, including 4.25 million transversions. We used this SNP set to call alleles for other canids from previous studies (Auton et al., 2013; Botigué et al., 2017; Freedman et al., 2014; vonHoldt et al., 2016; Wang et al., 2019a; Wang et al., 2013; Wang et al., 2019b; Zhang et al., 2014), and for the samples in the present study. For all but the Jiangxi sample, we used random allele calling, choosing not to determine heterozygous sites, as the sequencing depths for most individuals are low (~0.15x-15.3x, Table 1). We applied a filter where we ignored the first and last two base pairs of each fragment, required a base pair quality higher than 20, a fragment length of no less than 30, and mapping quality of no less than 30. The W2_Jiangxi sample was sequenced to 37x (Table 1), a high enough coverage to call heterozygotes confidently. Thus, we applied the software GATK 3.3 with the Unified Genotyper parameter to determine diploid calls. For the two Guizhou samples (W12_Guizhou and W13_Guizhou), we also made diploid calls with GATK using a similar process as for W2_Jiangxi to test whether results were consistent or not. After comparing all the analyses, we found the test results are similar to those obtained using random calling without heterozygous sites.

- QUANTIFICATION AND STATISTICAL ANALYSIS

- + Principal components analysis

To investigate the relationship of the newly sampled individuals to wolf and dog populations, we calculated pairwise allele-sharing distances among all pairs of wolf and dog populations (Cavalli-Sforza, 1997). We applied a principal components analysis (PCA) to the resulting pairwise distance matrix using SMARTPCA (version: 13050) (Patterson et al., 2012). For the gray wolves (31 individuals, including six new individuals sequenced in this study from China), we grouped populations by region:

America, Europe, Middle East, North Asia, Tibet, and Southern China. In the PCA, the six new samples are presented with a black edge and are slightly larger than the points for other samples (Figure 1B). The PCA also includes other wolves and select domesticated dogs, including breed dogs from across the world and indigenous dogs from South and North China. The first PC distinguishes between gray wolf and dog populations, while the second PC distinguishes between East Asian and European dogs (Figure S2). We changed the following options in the default ***PAR*** file: altnormstyle: No; outliermode: 1 and 2 for Figure 1B and Figure S2, respectively.

- + Phylogeny

We constructed the phylogenetic relationship of 31 gray wolves (*Canis lupus*), one ancient wolf from Taimyr, two coyotes (*Canis latrans*), two jackals (*Canis aureus*), one red wolf (*Canis rufus*), one dhole (*Cuon alpinus*), and one Andean fox (*Lycalopex culpaeus*) using the MEGA-CC (Compute Core) for Linux systems (https://megasoftware.net/) (Kumar et al., 2016). The MEGA-Proto requires two setting files (.mao) – one is for generating a Maximum Likelihood phylogeny and the other is for generating a Neighbor-Joining phylogeny. Support values of each node were inferred using 1000 rapid bootstrap replicates, where all other settings are set to the defaults. The ***fasta*** file for the 39 individuals was converted from the EIGENSOFT format using a customized script, and degenerate base symbols were used to represent the heterozygotes.

- + f3-statistics

For f3 statistics, we use the same dataset as shown in Figure S2, but including the Jackal. We measured the shared genetic drift between each newly sequenced wolf (X) and other dogs, gray wolves, and the Jackal (Y). We computed statistics of the form *f3(X, Y; Dhole)* using qp3Pop (version: 412), which measures the shared genetic drift between populations X and Y since their separation from an outgroup (*Dhole*) (Raghavan et al., 2014). After ranking the f3 results, we drew a scatter plot with error bars for the six new samples (Figure S5).

- + D-statistics

We used *D*-statistics (Green et al., 2010; Meyer et al., 2012; Patterson et al., 2012) of the form *D(Fox, Test; X, Y)* and *D(Fox, X; Test, Y)* to formally test the relationship these samples have with different wolf populations using qpDstat (version: 712), where X and Y are 15 previously published wolves and Test are each of the six newly sequenced gray wolves. We divided the results into 12 sub-tables (Table S3 and S5), and the results were highlighted according to the magnitude of the Z values. We also used *D(Fox, Jackal/Dhole; Test, Jackal/Coyote/Red Wolf/Zhejiang)* to assess the ancient genetic component in the Zhejiang wolf (Table S6), where Test are each of the Dhole, Coyote, Red wolf, six newly sequenced wolves and 14 previously published wolves.

- + TreeMix

We applied TreeMix (v.1.13) (Pickrell and Pritchard, 2012) to investigate the relationship between the newly sequenced samples and wolf and dog populations. TreeMix determines population structure using maximum likelihood trees and allows for both population splits and potential gene flow by using genome-wide allele frequency data and a Gaussian approximation of genetic drift. To further investigate how well the tree model fits the data, we visualized the matrix of residuals for the tree model with no admixture. We test trees for zero, one, and two migration events (m). The maximum-likelihood tree for m = 0 (Figure S4) is based on 39 canids excluding dogs. Figure S6 and S7 are based on all canids and m = 0. Figure 2 and Figure S8 are based on all canids with m = 1 and m = 2, respectively. To assess how well supported the Treemix phylogeny is, each node was inferred using 1000 rapid bootstrap replicates, with all other settings set to default parameters. To visualize the tree and residual plot, we used the R script plotting_funcs.R, and the ***plot_tree*** and ***plot_resid*** functions, which are provided with the source code for Treemix (https://github.com/joepickrell/pophistory-tutorial/tree/master/example2).

- + F4-ratio test

In the D-statistic analyses, we observed that the Zhejiang wolf showed patterns indicating ancestry from a canid population that separated from wolves earlier than the dhole separated from wolves. To estimate the proportion of ancestry in the Zhejiang wolf that was contributed by admixture with a population more archaic than the dhole, we use the F4-ratio test, which provides an unbiased estimate of the admixture proportion (Reich et al., 2011). We used qpF4ratio (v1.0) from the ADMIXTOOLS software package (Patterson et al., 2012). We use the dhole and fox as the two source populations for the wolves (X), assuming an unrooted tree (Figure S9). Then, we expect the admixture proportion, α, in the f4-ratio test to be given by the following equation, where X is each gray wolf in turn.

$$\frac{f_4(Dhole,\ Jackal;\ Coyote,\ X)}{f_4(Dhole,\ Jackal;\ Coyote,\ Andean\ Fox)}$$

- + Admixture Graph

We used qpGraph (version: 6065) from the ADMIXTOOLS packages (Patterson et al., 2012) to test all possible relationships between the select individuals representing the major branches for canids. We began with a base graph using three samples (Andean_fox, Dhole and Ancient_Taimyr). Then we proceeded by attempting to fit the selected gray wolf samples (Gray_Wolf_Iberia, Gray_Wolf_Indian, W9_Heilongjiang, W7_Zhejiang and Gray_Wolf_Great_Lakes) in turn. If there are no models that fit, we change the order of addition and repeat the analysis.

We added Gray_Wolf_Iberia to all possible nodes of basal Admixture Graph either as a simple branch without mixture, or as a mixture between two branches. All together, we identified two models that fit the data (maximum $|Z|<3$, Figure S10). We then added Gray_Wolf_Indian to all possible nodes of these two graphs (Figure S10), either as a simple branch without mixture, or as a mixture between two branches. We

identified two models that fit the data (maximum |Z|<3, Figure S11). Adding W9_Heilongjiang to all possible nodes of the two graphs that fit the data for Gray_Wolf_Iberia and Gray_Wolf_Indian (Figure S11), we identified only one model that fit the data (maximum |Z|<3, Figure S12). We added W7_Zhejiang to all possible nodes of this graph (Figure S12) and identified one model that fit the data (maximum |Z|<3), Figure S13) We finally added Gray_Wolf_Great_Lakes to the previous graph (Figure S13) and identified only one model that fit the data (maximum |Z|<3, Figure S14).

We additionally tested adding other canids to the admixture graph, but no graph fit the data well (i.e. all maximum |Z|>3). From the final admixture graph (Figure S14), we confirmed patterns similar to that observed in other analyses and we estimated a similar admixture proportion (14%) for deep ancestry in W7_Zhejiang (Figure S14).

- DATA AND SOFTWARE AVAILABILITY

Sequence data for six gray wolf genomes has been submitted to the Genome Sequence Archive (http://gsa.big.ac.cn/) under accession number PRJCA001135. The SNP set will be made available on the iDog database (http://bigd.big.ac.cn/idog/).

References

Auton, A., Li, Y.R., Kidd, J., Oliveira, K., Nadel, J., Holloway, J.K., Hayward, J.J., Cohen, P.E., Greally, J.M., Wang, J.*, et al.* (2013). Genetic Recombination Is Targeted towards Gene Promoter Regions in Dogs. Plos Genetics *9*.

Botigué, L.R., Song, S., Scheu, A., Gopalan, S., Pendleton, A.L., Oetjens, M., Taravella, A.M., Seregély, T., Zeeb-Lanz, A., Arbogast, R.-M.*, et al.* (2017). Ancient European dog genomes reveal continuity since the Early Neolithic. Nature Communications *8*, 16082.

Briggs, A.W., Stenzel, U., Johnson, P.L., Green, R.E., Kelso, J., Prufer, K., Meyer, M., Krause, J., Ronan, M.T., Lachmann, M., *et al.* (2007). Patterns of damage in genomic DNA sequences from a Neandertal. Proc Natl Acad Sci U S A *104*, 14616-14621.

Cavalli-Sforza, L.L. (1997). Genetic and Cultural Diversity in Europe. Journal of Anthropological Research *53*, 383-404.

Dabney, J., Knapp, M., Glocke, I., Gansauge, M.T., Weihmann, A., Nickel, B., Valdiosera, C., Garcia, N., Paabo, S., Arsuaga, J.L., *et al.* (2013). Complete mitochondrial genome sequence of a Middle Pleistocene cave bear reconstructed from ultrashort DNA fragments. Proc Natl Acad Sci U S A *110*, 15758-15763.

Dabney, J., and Meyer, M. (2012). Length and GC-biases during sequencing library amplification: A comparison of various polymerase-buffer systems with ancient and modern DNA sequencing libraries. Biotechniques *52*, 87-+.

Freedman, A.H., Gronau, I., Schweizer, R.M., Ortega-Del Vecchyo, D., Han, E., Silva, P.M., Galaverni, M., Fan, Z., Marx, P., Lorente-Galdos, B., *et al.* (2014). Genome sequencing highlights the dynamic early history of dogs. PLoS Genet *10*, e1004016.

Green, R.E., Krause, J., Briggs, A.W., Maricic, T., Stenzel, U., Kircher, M., Patterson, N., Li, H., Zhai, W., Fritz, M.H., *et al.* (2010). A draft sequence of the Neandertal genome. Science *328*, 710-722.

John, J.S. (2011). SeqPrep (https://github.com/jstjohn/SeqPrep).

Kircher, M., Sawyer, S., and Meyer, M. (2012). Double indexing overcomes inaccuracies in multiplex sequencing on the Illumina platform. Nucleic Acids Res *40*, e3.

Kumar, S., Stecher, G., and Tamura, K. (2016). MEGA7: Molecular Evolutionary Genetics Analysis Version 7.0 for Bigger Datasets. Mol Biol Evol *33*, 1870-1874.

Li, H., and Durbin, R. (2009). Fast and accurate short read alignment with Burrows-Wheeler transform. Bioinformatics *25*, 1754-1760.

Marsden, C.D., Ortega-Del Vecchyo, D., O'Brien, D.P., Taylor, J.F., Ramirez, O., Vila, C., Marques-Bonet, T., Schnabel, R.D., Wayne, R.K., and Lohmueller, K.E. (2016). Bottlenecks and selective sweeps during domestication have increased deleterious genetic variation in dogs. P Natl Acad Sci USA *113*, 152-157.

Meyer, M., and Kircher, M. (2010). Illumina sequencing library preparation for highly multiplexed target capture and sequencing. Cold Spring Harb Protoc *2010*, pdb prot5448.

Meyer, M., Kircher, M., Gansauge, M.T., Li, H., Racimo, F., Mallick, S., Schraiber, J.G., Jay, F., Prufer, K., de Filippo, C.*, et al.* (2012). A High-Coverage Genome Sequence from an Archaic Denisovan Individual. Science.

Patterson, N., Moorjani, P., Luo, Y., Mallick, S., Rohland, N., Zhan, Y., Genschoreck, T., Webster, T., and Reich, D. (2012). Ancient admixture in human history. Genetics *192*, 1065-1093.

Pickrell, J.K., and Pritchard, J.K. (2012). Inference of population splits and mixtures from genome-wide allele frequency data. precedingsnaturecom *http://precedings.nature.com/documents/6956/version/1*.

Raghavan, M., Skoglund, P., Graf, K.E., Metspalu, M., Albrechtsen, A., Moltke, I., Rasmussen, S., Stafford, T.W., Jr., Orlando, L., Metspalu, E.*, et al.* (2014). Upper

Palaeolithic Siberian genome reveals dual ancestry of Native Americans. Nature *505*, 87-91.

Reich, D., Patterson, N., Kircher, M., Delfin, F., Nandineni, M.R., Pugach, I., Ko, A.M., Ko, Y.C., Jinam, T.A., Phipps, M.E.*, et al.* (2011). Denisova admixture and the first modern human dispersals into Southeast Asia and Oceania. Am J Hum Genet *89*, 516-528.

vonHoldt, B.M., Cahill, J.A., Fan, Z., Gronau, I., Robinson, J., Pollinger, J.P., Shapiro, B., Wall, J., and Wayne, R.K. (2016). Whole-genome sequence analysis shows that two endemic species of North American wolf are admixtures of the coyote and gray wolf. Sci Adv *2*, e1501714.

Wang, G.D., Shao, X.J., Bai, B., Wang, J.L., Wang, X.B., Cao, X., Liu, Y.H., Wang, X., Yin, T.T., Zhang, S.J.*, et al.* (2019a). Structural variation during dog domestication: insights from gray wolf and dhole genomes. National Science Review *6*, 110-122.

Wang, G.D., Zhai, W.W., Yang, H.C., Fan, R.X., Cao, X., Zhong, L., Wang, L., Liu, F., Wu, H., Cheng, L.G.*, et al.* (2013). The genomics of selection in dogs and the parallel evolution between dogs and humans. Nature Communications *4*, 1860-1860.

Wang, G.D., Zhai, W.W., Yang, H.C., Wang, L., Zhong, L., Liu, Y.H., Fan, R.X., Yin, T.T., Zhu, C.L., Poyarkov, A.D.*, et al.* (2016). Out of southern East Asia: the natural history of domestic dogs across the world. Cell Res *26*, 21-33.

Wang, X., Zhou, B.W., Yang, M.A., Yin, T.T., Chen, F.L., Ommeh, S.C., Esmailizadeh, A., Turner, M.M., Poyarkov, A.D., Savolainen, P.*, et al.* (2019b). Canine transmissible venereal tumor genome reveals ancient introgression from coyotes to pre-contact dogs

in North America. Cell Res.

Zhang, W., Fan, Z., Han, E., Hou, R., Zhang, L., Galaverni, M., Huang, J., Liu, H., Silva, P., Li, P.*, et al.* (2014). Hypoxia adaptations in the grey wolf (*Canis lupus chanco*) from Qinghai-Tibet Plateau. PLoS Genet *10*, e1004466.